A COMFORT-BASED CONTROL STRATEGY IN BUILDINGS USING AN INFRARED CAMERA

A Thesis

Presented in Partial Fulfillment of the Requirements for the

Degree of Master of Science

with a

Major in Mechanical Engineering

in the

College of Graduate Studies

University of Idaho

by

Jubin George Mathai

Major Professor: Ralph Budwig, Ph.D.

Committee Members: L. Damon Woods, Ph.D.; Kamal Kumar Ph.D.

Department Administrator: Steven Beyerlein, Ph.D.

May 2020

AUTHORIZATION TO SUBMIT THESIS

This thesis of Jubin George Mathai, submitted for the degree of Master of Science with a Major in Mechanical Engineering and titled “A COMFORT-BASED CONTROL STRATEGY IN BUILDINGS USING AN INFRARED CAMERA," has been reviewed in final form. Permission, as indicated by the signatures and dates given below, is now granted to submit final copies to the College of Graduate Studies for approval.

Major Professor: _____ Date: _____
Ralph Budwig, Ph.D.

Committee Members:

_____ Date: _____
L. Damon Woods, Ph.D.

_____ Date: _____
Kamal Kumar, Ph.D.

Department Administrator:

_____ Date: _____
Steven Beyerlein, Ph.D.

ABSTRACT

This proof-of-concept study focuses on the feasibly of using a low-cost infrared camera to determine comfort conditions indoors. There are six parameters that govern the thermal comfort of an occupant which are clothing levels, metabolic activity, air velocity, relative humidity, air temperature, and the most importantly the mean radiant temperature (MRT). Almost 40% of our thermal perception of indoor surroundings occurs through radiation. The conventional thermostat measures only air temperature as a control parameter. Several studies show that air temperature alone as a control parameter causes occupant discomfort, reduces productivity, and increases energy usage in buildings. The main energy driver in buildings is thermal comfort. In this study, a comfort-based control strategy was developed based on Fanger's Predicted Mean Vote (PMV) method. The infrared camera's surface temperature readings were validated with thermocouple measurements and were found to be in the range of $\pm$1.23°F. We developed a spreadsheet tool in Excel to determine MRT and PMV values which agreed with the Center of Built Environment's thermal comfort tools. Infrared images combined with machine learning techniques performed occupant detection. Energy models were used to predict energy savings and uncomfortable hours in three different climate zones in the United States with a PMV based control in comparison to conventional control. The simulation results indicated that the PMV based control maintained thermal comfort across all the locations, significantly lowered the overcooling issues dominant in conventional control, and had energy-savings at the Tampa, Florida location.

ACKNOWLEDGEMENTS

This thesis work would not be completed without the guidance and help that I received from the people whom I met during this journey. I am extremely grateful to Dr. Ralph Budwig for his invaluable guidance and support throughout my master's study and research. I thank him for introducing me to scientific research and steering me in the right direction. I thank Dr. Damon Woods for his relentless encouragement, patience, and insights in every difficult situation that I faced in this study. I learned a lot about energy efficiency in the built environment under his mentorship. Thank you to Dr. Kamal Kumar for reviewing my work and for the insightful questions.

I would like to thank Andrew Brewick, the GSSP staff and Professors who taught my coursework's in the master's program, for their lectures and research works have inspired me in the completion of my master's degree. This project was funded by Avista Utilities and I especially thank Randy Gnaedinger, Carlos Limon, and Natasha Jostad in their continuous support throughout the project phase. I thank Elizabeth Cooper who brought me to the IDL from the U of I, Moscow campus. I had a wonderful time working with the IDL team headed by Ken Baker and alongside Dr. Damon Woods, Dylan Agnes, and Lyndsay Watkins. Thanks for all your help and encouragement. I thank Idaho Power and the North West Energy Efficiency Alliance in supporting with funds and exciting projects. To all my friends, thank you for the memorable moments during this journey.

I am sincerely humbled by the consistent support of my parents, who have perpetually loved, cared, and sacrificed for me. I am forevermore indebted to my sisters who have remained a beacon of light during my darkest hours.

DEDICATION

To my family, Mathai Varghese (Father), Nirmala Mathai (Mother), Shanti Chechi (Elder Sister) & Jerin (Younger Sister). Thank you for believing in me and always inspiring me to do my best.

TABLE OF CONTENTS

LIST OF TABLES

LIST OF FIGURES

CHAPTER 1 : **A COMFORT-BASED CONTROL STRATEGY IN BUILDINGS USING AN INFRARED CAMERA**

1.1 Introduction

From an ancient civilization of humans who spend most of their time outdoors, modern-day humans spend 90% of their time indoors. The United States that represents 4.27% of the world's population consumes 19% of the world's energy, of which 41% accounts for the built environment. Due to the rapid industrialization and modernization of the world, the built environment is one of the fastest growing sectors. The primary objective of a building is to keep people inside thermally comfortable and safe from the harsh environments outside. But energy is required to keep us thermally comfortable indoors. Current practices and building systems are primarily focused on achieving energy efficiency. Thermal comfort is not a product that can be bought and it is often confused by consumers with energy-efficient systems (Ng, 2019). The main energy driver in buildings is thermal comfort. Thermal comfort is defined as "that condition of mind which expresses satisfaction with the thermal environment" (ASHRAE, 2013). The comfort of occupants in buildings has economic implications beyond the cost of energy required to condition the space and has strong correlations to human performance, health, and well-being (Brager, Zhang, & Arens, 2015).

In modern buildings, thermal comfort depends mainly on the electro-mechanical systems that maintain the temperature indoors. The thermal comfort guideline used for indoor environmental design is the ASHRAE-55 standard, which requires buildings that are mechanically conditioned to maintain at least 80% of its occupants to be comfortable within a space. However, various studies showed that most buildings do not meet this

criterion (Huizenga, Abbaszadeh, Zagreus, & Arens, 2006) (Karmann, Schiavon, Graham, Raftery, & Bauman, 2017). Temperature dead bands in practice are as small as 1-2°C in North America which often results in overcooling in summer and has significant energy cost (Brager, Zhang, & Arens, 2015). Over-cooling complaints are common in commercial buildings in the United States and account for substantial energy, environment, and financial costs (Mendell & Mirer, 2009) (Derrible & Reeder, 2015). From an analysis conducted by (Federspiel, 1998) from 23,500 occupants in 690 commercial buildings on the frequency of complaints, results indicated that the thermal sensation complaints (too hot or too cold) were the single biggest type of complaint. In a survey conducted by various researchers over common problems in buildings, thermal comfort was ranked by building occupants to be of greater importance (Arditi & Nawakorawit, 1999) (Frontczak & Wargocki, 2011).

Due to rapid mechanization and modernization, the built environment is one of the fastest-growing sectors and is adapting to social needs at large. 70% of the world's population is estimated to be located in urban areas by 2050 according to the United Nations. Urbanized areas are increasing worldwide and according to world development indicators, 85% of the population will be located in developing countries in 2030. Around 70% of energy worldwide, is consumed by buildings for air-conditioning and lighting purposes (Rupp, Vásquez, & Lamberts, 2015). Over 80 studies indicated that the highest potential to reduce global baseline emissions by 2020 cost-effectively, lies in the built environment by approximately 29% (Levine, et al., 2007).

The United States consumes 19% of the world's energy, of which 41% of the energy consumed is by the built environment overtaking transportation and industrial

sectors. 74% of the electricity produced in the United States is consumed by buildings and responsible for 40% of the carbon dioxide emissions and 7.4% globally (Reddy, Kreider, Curtiss, & Rabl, 2017). With the growing population, the need for comfortable and energy-efficient buildings is on the rise.

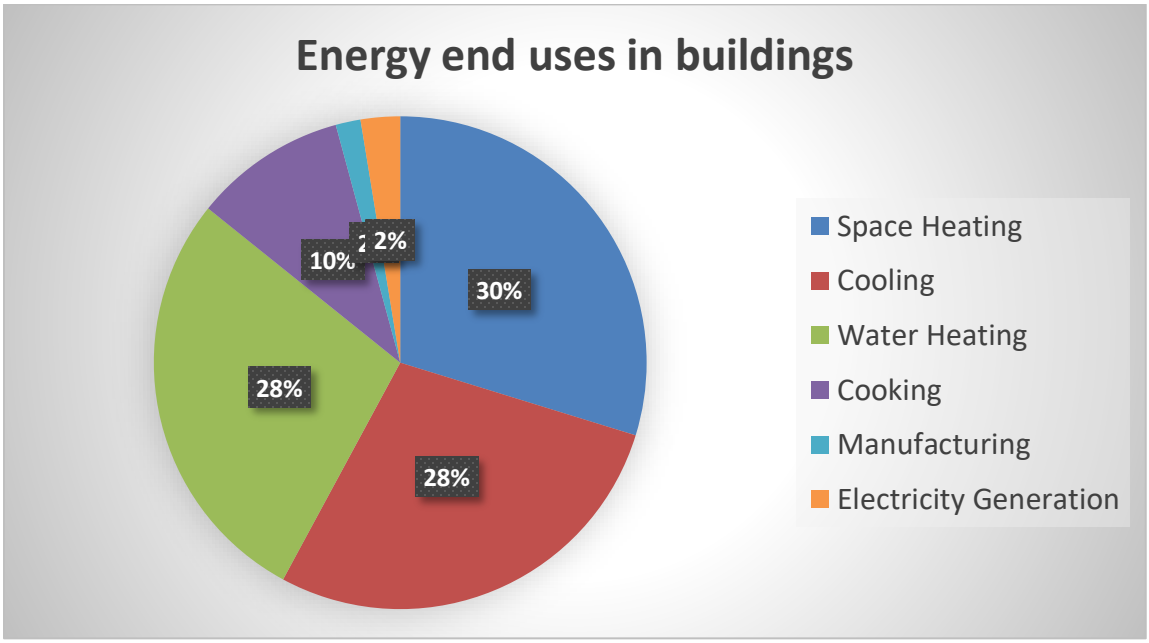

Figure 1.1: U.S commercial energy consumption by end-use, 2012 (U.S. Energy Information Administration, 2016)

Figure 1.1 shows end energy usage in the commercial buildings sectors in the U.S. The energy required for space heating and cooling combined accounts for 58%. The primary driver of energy in buildings is to maintain human thermal comfort. Several researchers address the issues of thermal comfort in buildings and propose solutions in their studies with comfort centered-control algorithms for space conditioning (Liang & Du, 2005) (Donaisky, Oliveira, Freire, & Mendes, 2007) (Duan, Ding, Shi, Xiao, & Duan, 2011) (Syafril, Yashiro, Khan, Koshizuka, & Sakamura, 2015) (Konis & M.Annavaram, 2017) (Aghniaey & M.Lawrence, 2018) (Zhe Wang, et al., 2018) The

primary purpose of the energy-consuming systems in buildings is to provide comfortable and healthy environment for its occupant's. The thermal discomfort of the people in the buildings leads to productivity loss at work which has strong economic correlations that far exceed the cost of energy to operate the buildings (Brager, Zhang, & Arens, 2015).

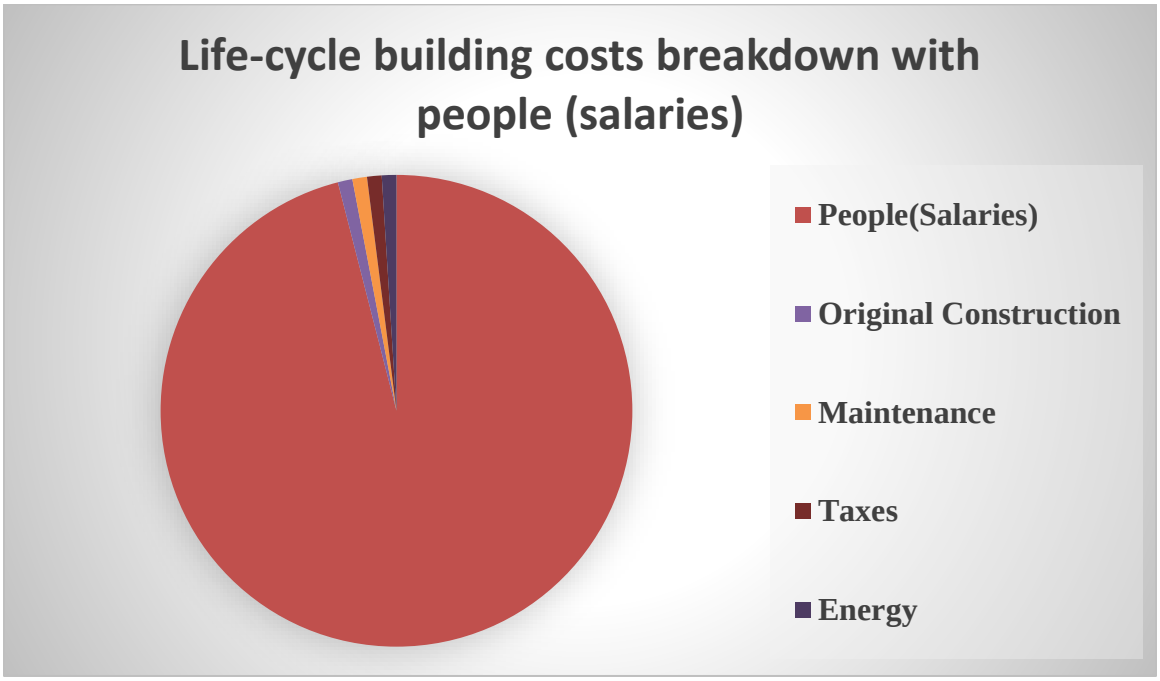

Figure 1.2: Life cycle building costs breakdown with salaries of people (Tom, 2008)

Figure 1.2 shows life cycle building costs breakdown with the salaries of the people included. Since the oil crisis in the 1970s, energy reduction has been of great importance in buildings. Most often, the facility management team becomes so focused on saving energy, neglecting the primary goal to which the building was originally constructed. If we add the salaries of the people that work in the building to its life cycle cost, the salaries of the people living in the building dwarf any other building cost (Tom, 2008). The "human factor costs far outweigh the energy costs in buildings by more than a factor of 100" (Bean, 2014).

In a typical office, some people are cold, and some are hot due to individual biological differences. If an occupant is too hot or too cold within a space, the individual will keep adjusting the thermostats to maintain comfort. Due to such frequent thermostat adjustments, potential energy saving setpoints adjusted by the facility manager is reduced. If the thermal comfort needs of occupants in the space are addressed, energy efficiency will follow. There needs to be a balance between thermal comfort and energy efficiency for us to achieve a sustainable built environment.

1.2 Radiative Heat Transfer

Radiative heat transfer is the most common energy transfer experience that we feel around us in daily life. The sun's energy in the form of electromagnetic waves is absorbed and scattered, thereby heating everything around us. It allows us to sense and see everything around us as light or heat. All objects around us emit electromagnetic radiation. The complex relations between the energy levels of atoms and molecules that make up matter govern the laws of radiative emission. Radiation transfer plays an important role in many engineering applications and is important even at room temperature. Cold window surfaces can have a chilling effect as the body radiates heat to them and similarly, the warming effect of sunshine can be felt even in winter (Howell, Siegel, & Menguc, 2011). Atmaca conducted a simulation study and results indicated thermal discomfort for occupants in buildings that were placed closer to relatively hot surfaces (Atmaca, Kaynakli, & Yigit, 2007).

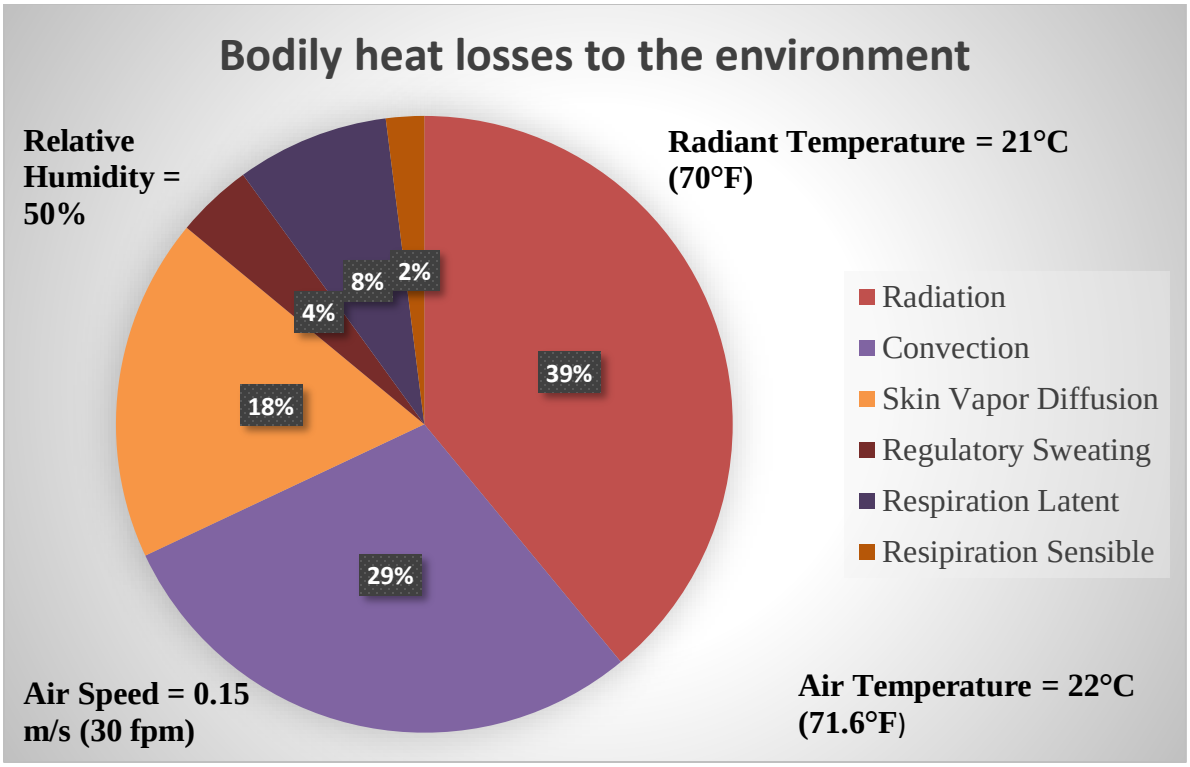

Figure 1.3: Body heat loss to the environment in typical winter clothing, standing relaxed individual (Mora & Bean, 2018)

Figure 1.3 shows bodily heat losses to the environment in typical winter clothing for a standing relaxed individual. Of the three main modes of human heat exchange (radiation, convection, and metabolically) the one that has the highest influence that affects our perception of comfort is radiation (Huizenga, Zhang, & Arens, 2001). Radiation accounts for the highest heat loss and accounts for almost 40% of the way we thermally feel and exchange heat.

Radiation exchanged between the human body and the surrounding room surfaces play a key role in determining thermal comfort. Occupants frequently experience heterogenous radiation that causes discomfort mainly through cold windows, non-uniform surface temperatures, or through high-intensity artificial sources in the room.

Radiant heat transfer does not directly affect the indoor air temperature. The longwave radiation reheats the surrounding surfaces, which indirectly heat the air**.** Through radiation, the heat exchange between two internal surfaces is largely impacted by the view factor between the heat emitting surface, the receiving surface, and the emissivity of the surfaces. View or angle factor relates to the geometrical shape, size and distance between two objects. The sum of the view factors between the person and surrounding room surfaces is equal to one (Babiak, Olesen, & Petras, 2009).

"The mean radiant temperature in relation to a person in a given body and clothing placed at a given point in a room is defined as that uniform temperature of surroundings, modeled as black-body surfaces, which will give the same radiant heat loss from the person as the actual case under study" (Fanger, 1970). Mean radiant temperature (MRT) is an important parameter that govern human energy balance (Thorsson, Lindberg, Eliasson, & Holmer, 2007) (EmanueleNaboni, MarcoMeloni, SilviaCoccolo, JérômeKaemp, & Jean-LouisScartezzini, 2017). MRT is a combination of long-wave and short-wave radiations. Various studies have been conducted on the assessment of MRT indoors. Palmer discusses and compares two such methods to calculate MRT (Palmer & Chapman, 2000). Tredre conducted an MRT assessment study with reference to a point in the room to approximate the heat load on an occupant in the room (Tredre, 1965). The value of MRT is dependent on the point of reference used for measurement. Hence view factor is important in the calculation of radiative heat exchange between the person and surrounding surfaces.

Fanger developed view factor correlations by means of large sets of graphs for rectangular surfaces (Fanger, 1970). Dunkle using a mechanical integrator performed

measurements to derive empirical relations for view factors from points on various surfaces to standing or seated persons (Dunkle, 1963). Several researchers have discussed different approaches to calculating view factors (Burt, Terjung, & O'Rourke, 1982) (Davies, 1984) (Cannistraro, G.Franzitta, Giaconia, & Rizzo, 1992) (Narayana, 1998) (Bahadori, Zendehboudi, Zahedi, & Jamili, 2014). However, in indoor thermal studies the common assumption is to omit the measurement of MRT and assume MRT to be equal to the air temperature (Chaudhuri, Soh, Bose, Xie, & Li, 2016). The main reason standard practice avoids the measurement of MRT is due to the complex MRT measurement techniques and the hypothesis that the condition indoors has uniform radiation fluxes and temperatures (Noémi Kántor, 2011) (Chaudhuri, Soh, Bose, Xie, & Li, 2016). MRT and air temperatures can vary especially in buildings that have large facades. The primary focus of this paper is the mean radiant temperature, an important parameter in thermal comfort metrics whose calculation requires radiometric data of the space that can be analyzed by an IR camera.

1.3 Infrared Cameras

The Infrared camera (IR) camera was originally developed for military purposes and its applications at present have extended to the fields of medicine, electrical installations, astronomy, building maintenance, and energy audits. IR cameras are predicted to be an integral part of automotive, environmental control and smart buildings and are reviewed in detail by (Kylili, Fokaides, Christou, & Kalagirou, 2014) (Lucchi, 2018). Several researchers use infrared thermographic techniques to investigate the thermal performance of buildings (both existing and under construction) and found positive results in its applications (Tim, Counsell, & Gill, 2013) (Rossano, M.Tonelli, &

Chiogna, 2015) (Tejedor, Casals, MartaGangolells, & Roca, 2017). All objects around us emit infrared radiation. Infrared is the region of the electromagnetic spectrum that has longer wavelengths than the visible light than humans can see. An IR camera detects and calculates the infrared radiation of the objects. IR emissions can only be sensed by humans as heat. An IR camera assigns a false range of colors that humans can perceive as IR energy. An IR camera is a non-contact measurement method that is ideal for measuring indoor surface temperatures.

Alfano conducted a study to compare different methodologies and instruments used to measure the mean radiant temperature as reported in the ISO standard 7726. The method of determining MRT based on view factors by using a thermal camera or radiation thermometers showed good reliability (Alfano, Isola, Palella, Riccio, & Russi, 2013). Due to problems of emissivity, calibration, focus, placement and reflections, IR cameras are mostly restricted to qualitative rather than quantitative assessments (Porras-Amores, Mazarron, & Canas, 2013). Several researchers study techniques that can be used for accurate measurements in quantitative thermography (Marinetti & Cesaratto, 2012). Datcu conducted an experimental study on using infrared thermograph for surface temperature measurements and results showed good agreement between thermocouple temperatures and the infrared cameras temperature measurements (Datcu, Ibos, Candau, & Matteï, 2005). Several studies also proved that an IR camera can be used to detect an occupant in space using object detection algorithms (Benezeth, Emile, Laurent, & Rosenberger, 2008) (Budzan, 2015) (Gomez, Conti, & Benini, 2018) (Akula, Shah, & Ghosh, 2018). For a building management system this provides unique data to building operators and can drive building systems more efficiently. Occupancy data can provide

crucial information to the HVAC system on ventilation requirements. Occupancy sensors are now mandatory in several energy codes for various buildings and system types, e.g. Washington's new energy code (WEC C403.1.6.1). With recent price drops in IR cameras, the idea of incorporating IR cameras into the energy management systems in buildings poses several advantages to building performance.

The use of IR cameras has broadened and have been used as a means of determining thermal comfort in occupants to achieve better building operational standards. Fokaides proves a method to measure indoor air temperature using IR thermography within a 1% difference with thermocouple measurement (A.Fokaides, AndriusJurelionis, LauraGagyte, & A.Kalogirou, 2016). Cosma used a thermographic camera to model human thermal comfort at transient conditions indoors (Cosma & Simha, 2018). Similar studies have been conducted by several researchers using thermal cameras to model thermal comfort (Mihai, et al., 2014) (Ranjan & Scott, 2016) (Pavlin, et al., 2017). The Princeton University research team has developed a Spherical Motion Average Radiant temperature (SMART) sensor that measured mean radiant temperature with respect to an occupant. This device is a combination of a single infrared sensor and a range finder. The smart sensor works well in an enclosed environment with radiantly active walls, but its effectiveness in open offices and integration with a building management system is yet to be understood (Guo, Teitelbaum, Read, & Meggers, 2017). As opposed to an IR sensor, an IR camera can measure surface temperatures over a wide spatial resolution in a single frame, which makes it ideal for measuring mean radiant temperature.

1.4 Thermal Comfort

Typically, there are two types of approaches that address thermal comfort in an indoor environment, the rational and the adaptive approach. The rational approach is widely accepted and used in international standards such as ASHRAE-55 and EN ISO-7730. It is based on theoretical human heat exchange calculations performed by P.O Fanger in the mid-latitude climatic regions in North America and Northern Europe. The adaptive approach is based on an individual's responsibility and is only a function of the outdoor air temperature. The adaptive approach for thermal comfort lacks in the measurement of the mean radiant temperature which governs almost 40% of the occupant's comfort. The adaptive approach is more suited to naturally ventilated buildings.

"A rational calculation of heating and air-conditioning systems must begin with the conditions for comfort" (Fanger, 1970). Thermal comfort is a state of mind that is experienced and perceived by us through our senses. It is a subjective experience. Our approach to calculating optimal thermal comfort in a room is based on Fanger's PMV model. The thermal comfort approach developed by P.O. Fanger is a steady-state model. This method can be applied to artificially conditioned spaces particularly to North America and European countries. The method is based on predicting the mean vote on an ordinary rating scale of thermal comfort that ranges from -3 to +3. The comfort metrics can be calculated in two ways: either as a Predictive Mean Vote (PMV) or as a Percentage of Population Dissatisfied (PPD). PMV is the most widely used thermal comfort index for indoor environmental quality studies.

The hypothalamus, a small region of the brain plays a crucial role in regulating the body's temperature within a range from 36°C to 38°C. The hypothalamus is the operator and the pituitary gland connected to the hypothalamus is the internal thermostat. It is responsible for controlling the core body temperature. This detailed regulation process is discussed by (Bean, 2012). Thermal regulatory functions in our body are complex processes and air-temperature alone as a control parameter in thermostats is a poor determinant in the evaluation of thermal comfort of an occupant in space. In an office environment, the best possible appropriate approach in having a thermal satisfaction with the surroundings is a set of conditions acceptable to most occupants in space. Fanger's PMV-PPD method considers six parameters that govern thermal comfort in humans and calculates maximum acceptable levels to which occupants remain comfortable in space. The PMV is the result of a comfort equation developed by Fanger using results from numerous climate control experiments. The equation establishes a link between the deviation from the minimum load on occupant's thermoregulatory systems (sweating, Vasco-constriction, vasodilation) and thermal comfort vote and depending on the load, more the PMV deviates from 0. To predict thermal sensation vote, PMV is scaled on a seven-point scale (-3 cold, -2 cool, -1 slightly cool, 0 neutral, +1 slightly warm, +2 warm, +3 hot) and signifies the thermal comfort levels (Fountain, Huizenga, & Charlie, 1995). A PMV of 0 indicates thermal neutrality. The PMV approach considers the combination of conditions satisfying the comfort equation essential for optimal comfort for occupants.

Thermal comfort is a combination of two personal and four environmental factors, the environmental factors are air temperature, air velocity, relative humidity, and the

mean radiant temperature. The personal factors include activity and clothing levels. The below paragraphs discuss the six governing parameters in determining thermal comfort in an occupant based on Fanger's approach and the values we measured and assumed in our study. The six governing factors are metabolic rate, clothing level, air temperature, mean radiant temperature, air velocity, and relative humidity. The below sections discuss the parameters in detail.

Metabolic Rate

The human body is a heat engine. It follows conservation of energy that is metabolic heat must be released at the rate at which it is generated. Metabolic rate is expressed as "Met" and is 58.2 watts per square meter of skin surface area. Higher the activity levels higher will be the metabolic rates. Table 1.1 shows metabolic activity rates for typical activities in the office and miscellaneous occupations.

Table 1.1: Metabolic Rates for Typical Tasks (ANSI/ASHRAE, 2013)

Metabolic Rate			
Office Activities	Met units	W/m^2	$Btu/h.ft^2$
Reading, seated	1	55	18
Writing	1	60	18
Typing	1.1	65	20
Filing, seated	1.2	70	22
Filing, standing	1.4	80	26
Walking about	1.7	100	31
Lifting/ Packing	2.1	120	39

Clothing Level

The insulation layer that keeps your heat trapped near your skin is clothing. It is expressed in terms of clo units. It is an index that uses a number to define all the effects of different clothes on wearers. Table 1.2 shows clo values for different clothing ensembles. Typically, clo value of 0.5 resembles summer wears and a clo value of 1 resembles winter wears.

Table 1.2: Clothing Insulation clo values for typical Ensembles (ANSI/ASHRAE, 2013)

Clothing Description	Garments Included	Icl, clo
Trousers	Trousers, short-sleeve shirt	0.57
	Trousers, long-sleeve shirt	0.61
Shorts	Walking shorts, short sleeve shirt	0.36
Skirts/ dresses	Knee-length skirt, short-sleeve shirt(sandals)	0.54
	Ankle-length skirt, long-sleeve shirt, suit jacket	1.1
Athletic	Sweatpants, long-sleeve sweatshirt	0.74

Air Temperature

It is also referred to as dry-bulb temperature. It is the temperature of the air measured around us. It is measured in Celsius or Fahrenheit. This parameter is the most widely used control parameter in a conventional thermostat.

Mean Radiant Temperature

MRT is the averaged surrounding surface temperatures in the room. It is measured in Celsius or Fahrenheit. The inclusion of MRT in building controls is important for determining better comfort conditions in space and is crucial especially to buildings with large windows. The primary focus in this study was the accurate calculation of the mean radiant temperature using an infrared camera in the PMV based control logic and to integrate with a building control.

Air Velocity

Air velocity is the speed with which air moves from point to point in space. Several researchers discuss the importance of air velocity on thermal comfort and correlated relative errors found in current practices (Srivajana, 2003) (Zhang, et al., 2007) (Kuru & Calis, 2017).

Relative Humidity

It is the amount of water vapor content in the air. It is measured in percentage. Studies conducted on the influence of humidity under steady-state and transient conditions are discussed by several researchers (Tanabe, Kimura, & Hara, 1987) (Jing, Li, Tan, & Liu, 2013) (Djamila, Chu, & Kumaresan, 2014) (Kuru & Calis, 2017).

P.O Fanger's comfort equation is a combination of these factors in order to achieve optimal thermal comfort. Out of the six parameters that govern thermal comfort, the most important is the mean radiant temperature as it has the highest influence to our perception of thermal comfort indoors. Due to biological differences, it is not possible to keep each individual comfortable in an artificial climate at the same time (JuntaNakano,

Tanabe, & Kimura, 2002). The PMV equation is a score that can be understood through the thermal sensation scale shown in Table 1.3. From PMV, percentage of people dissatisfied (PPD) can be determined. PPD predicts the percentage of people dissatisfied with the environment. PMV results indicate whether the indoor environment is comfortable or not.

Table 1.3: Thermal Sensation Scale (Ekici, 2013)

Thermal Sensation Scale		
PMV value	Scale	Comments
3	hot	intolerably warm
2	warm	too warm
1	slightly warm	tolerably uncomfortable, warm
0	neutral	comfortable
-1	slightly cool	tolerably uncomfortable, cool
-2	cool	too cool
-3	cold	intolerably cool

Table 1.3 shows the thermal sensation scale and comments that result from the combination of six thermal comfort parameters. The PMV ranges from plus three to minus three where plus three indicates the space being intolerably hot and minus three indicates the space is too cold. From Fanger's study, 5% of people in a space will be always dissatisfied with the thermal environment. A PMV-PPD scale would be an appropriate method to govern thermal comfort acceptable to the largest group of people in a mechanically conditioned space. Various studies state that mechanically conditioned spaces work well with PMV-PPD and can be used to evaluate thermal comfort (Ekici, 2013) (Yang, Yan, & Lam, 2014). Even though the PMV method has long existed in

literature and used for comfort evaluation studies, PMV based control strategy incorporated in building controls is hardly seen in practice.

1.5 Conventional Controls

Thermostats have evolved over time in functionality and serve as the primary control in determining the thermal comfort of the occupant in space. If an occupant is uncomfortable, they will keep adjusting the controls until a state of comfort with their surroundings is achieved or will persuade the building operator on the issue. Thus, potential savings are reduced in adjusting thermostat setpoints when occupants change them back. The lack of occupant satisfaction is the driving force behind thermostat adjustments.

Case studies conducted by researchers from the University of Helsinki and Lawrence Berkeley National Laboratory on the productivity of office workers showed savings up to $330 can be saved per employee by maintaining temperature setpoint within the range of 72°F and 77°F (Tom, 2008). Productivity decreased rapidly below or above this range. Chang conducted a gender-based study of understanding the effect of temperature on cognitive performance and results suggested that in gender-mixed workplaces, the productivity can be increased by setting the thermostat higher than current standards (Chang & Kajackaite, 2019). However, expanding thermostat setpoints are only feasible if comfort for the occupant is maintained. The single largest occupant driven variable in residential simulations at present is heating setpoints and has a significant impact on energy usage in homes (Metzger & Norton, 2014). Research has shown that a thermostat reset could result in savings of 4-7% of the building's annual energy consumption (Hoyt, Arens, & Zhang, 2014).

Present guidelines recommend proper setpoint adjustments for energy efficiency, but the information in relation to thermal comfort achieved by occupants in space is scarce (Kontes, Giannakis, horn, Steiger, & Rovas, 2017). At present, thermostats are programmable, adaptive, and expected to achieve efficiency. But case studies show that users do not properly operate the thermostat functions and energy savings fall short of their rated potential (Nevius, 2000) (Haiad, Peterson, Reeves, Hirsch, & Hirsch, 2004) (Michelle, et al., 2009) (Pritoni, Meier, Aragon, Perry, & Peffer, 2015). This led to the Environmental Protection Agency (EPA) suspend the energy star program for programmable thermostats (Huchuk, O'Brien, & Sanner, 2018). Newer generation indoor controls are the smart thermostats that maintain indoor temperatures more efficiently with the ability to use occupant data to govern thermal comfort in space. Several researchers have developed algorithms to optimize energy without sacrificing comfort with smart thermostats (Ham, MichelKlein, Tabatabaei, J.Thilakarathne, & Treur, 2016) (Pritoni, Salmon, Sanguinetti, Morejohn, & Modera, 2017). A potential flaw with smart thermostats especially when implemented for office buildings is that the control would assume only the needs of an individual in control and not be a representation of the thermal needs of the larger group in space (Ng, 2019). An ideal control would be focused primarily on occupant satisfaction and not energy efficiency. Both are inter-dependent for a sustainable built environment. If occupants in the space are thermally satisfied with their surroundings, the frequent thermostats adjustments will reduce thereby decreasing energy cost in conditioning. Hence, controls based on occupant satisfaction should be incorporated. Various HVAC setpoint adjustment studies proved a good relationship

between thermal comfort and energy efficiency (Kwong, Adam, & Sahari, 2014), (Hoyt, Arens, & Zhang, 2015).

The most widely used control parameter to achieve the state of thermal comfort indoors is the air temperature and several researchers suggest that dry-air bulb temperature alone as a determinant to thermal comfort is not adequate (Duan, Ding, Shi, Xiao, & Duan, 2011) (Kontes, Giannakis, horn, Steiger, & Rovas, 2017) (Woods, 2018) (Haiying, Olesen, & Kazanci, 2019) (Teitelbaum, et al., 2020). Most often, in indoor thermal studies, the common practice is to assume air temperature and mean radiant temperature to be equal (Olesen & Parsons, 2002) (Omer & Kilic, 2005) (Thomson, Garcia-Herrera, & Beniston, 2008) (Langner, Scherber, & Endlicher, 2014) (Walikewitz, Jänicke, Langner, Meier, & Endlicher, 2015) (Chaudhuri, Soh, Bose, Xie, & Li, 2016) (Zang, Xing, & Tan, 2019). This assumption in building systems indirectly causes huge occupant discomfort problems and leads to the mechanical systems to operate inefficiently. This has serious financial implications on the operational cost of the buildings due to the maintenance teams continuously addressing with the huge number of user comfort issues. The most important problem the building operation and maintenance team face are building design inefficiencies (Arditi & Nawakorawit, 1999). This highlights the need for MRT measurements and the incorporation of comfort in controls.

The measurement of the mean radiant temperature is not a direct method and is generally calculated with the combination of different methodologies and instruments. This is discussed in detail by reliability (Alfano, Isola, Palella, Riccio, & Russi, 2013).The most common type of surface temperature measurement techniques includes the globe thermometers, surface mounted thermocouples, and the infrared cameras. In

mean radiant temperature measurement, globe thermometers have been the gold standard in practice and serval researchers use this to determine MRT (Pablo, Salmerón, Ruiz, Sánchez, & Brotas, 2016) (Vargas-Salgado, Chiñas-Palacios, Aguila-León, & Alfonso-Solar, 2019). Teitelbaum conducted a study and results showed that the standard convection correction readings in globe thermometers are higher than the established readings which implies that all the past research works on globe thermometers could have been inaccurate (EricTeitelbaum, et al., 2020). The MRT measurement with respect to different locations indoors is not practical with globe thermometers and surface mounted thermocouples in real-time. The globe thermometer and the surface mounted thermocouples are point-radiation measuring devices and radiometric data of only the particular point in the room being measured can be obtained. The infrared camera is a non-contact measurement device and covers a wide range of spatial radiometric data of the surface being measured. This makes it a better technique for the measurement of the mean radiant temperature indoors. Occupant satisfaction within a building will be improvised largely with the inclusion of MRT in building controls and can also save energy. Therefore, a thermostat control strategy should focus on human thermal comfort so that the setpoints are not immediately changed after they are implemented.

Several researchers have found positive findings incorporating a PMV based control strategy in buildings (Park & Rhee, 2018). MacArthur was the first to propose a control strategy in buildings with PMV as its logic (MacArthur, 1986). Scheatzle used a PMV control algorithm to optimize energy (Scheatzle, 1991). Tse conducted simulation studies on the implementation of the PMV based control algorithm on an air handling unit and found superior performance over conventional thermostat setpoints (Tse & So,

2000). Laing showed PMV control parameters as a control logic can maintain the indoor temperature in comfort levels and also has the potential for energy savings (Liang & Du, 2005). Zang developed a thermal comfort system based on PMV using machine learning techniques and sensors connected together by the Internet of things (Zang, Xing, & Tan, 2019). Zang assumed the mean radiant temperature equal to the air temperature in the PMV calculation which can lead to inaccurate PMV value, especially for building with large facades. Zhao developed a PMV controlling system for the building based on the Internet of things (IoT) and Artificial intelligence (Zhao, Genovese, & Li, 2020). The control system uses a wet-blub globe thermometer for radiant measurement along with other IoT sensors. Wet-bulb globe thermometers are prone to errors in measurements, is a point radiation measurement device and are not a feasible method in building spaces, because they must be suspended in the middle of the room. Chaudhuri conducted a large database study involving 10,000 occupants covering 9 climate zones and 4 seasons on the effect of assuming mean radiant temperature equal to the air temperature showed that even a small difference in air temperature and MRT can lead to significant error in the determination of thermal comfort (Chaudhuri, Soh, Bose, Xie, & Li, 2016). Therefore, accurate measurement of MRT in the comfort control strategy for building controls is important.

While the theory of PMV based control in buildings has existed since the 1980s, the author is aware of only two published implementation efforts. The first author, Zang assumed MRT equal to air temperature (Zang, Xing, & Tan, 2019). The second author, Zhao used point radiation temperature measurements to estimate MRT (Zhao, Genovese, & Li, 2020). In our study entire occupant space surfaces were thermally imaged by an IR

camera and then view factor correlations were applied to obtain MRT. Our study focuses on obtaining a comfort-based control signal based on PMV for controlling indoor air temperature with emphasis on obtaining accurate MRT readings with the indoor surroundings. This study is a proof-of-concept of the practical implementation of a PMV based control using an IR camera in building controls. A comfort-based control strategy in buildings has a greater probability of remaining in place.

The objective of this study is to introduce a method to predict occupant comfort using a low-cost IR camera that incorporates MRT with respect to an occupant in the space. With the use of open-source software applications, we develop a methodology that addresses the occupant's comfort needs and energy savings through comfort control settings in buildings using Fanger's comfort model prescribed in ASHRAE Standard-55. As technologies and solutions are evolving rapidly towards a sustainable built environment, our aim is to develop and test the feasibility of the comfort-based control strategy in buildings. Furthermore, the same IR camera that is used to calculate MRT will also be applied for occupant detection. Finally, energy simulations were performed to compare the relations of thermal comfort conditions and energy savings of conventional air temperature thermostat setpoints versus PMV setpoints in three different climate zones across the United States.

CHAPTER 2 : **METHODS**

2.1 A Comfort Controlled Strategy in Buildings

In recent years, the availability, size, reduced cost, and enhanced capabilities of infrared cameras have fostered new application to a variety of measurement needs. With the availability of low-cost infrared cameras, we developed a method that can measure radiometric surface temperatures and detect occupancy in its field of view. Using Microsoft Excel and open source tools we incorporated thermal comfort parameters that can be used to drive HVAC systems in buildings. The below sections discuss the method we used to develop the process.

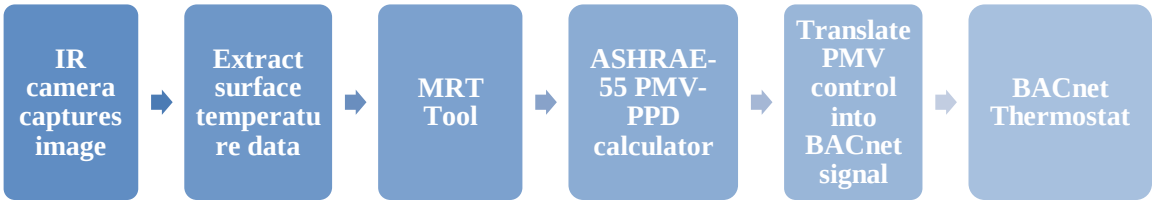

Figure 2.1: Block diagram for a comfort-based control strategy

Figure 2.1 shows the block diagram describing the method we used to obtain a comfort-based control strategy in buildings. Mean radiant temperature calculation and implementation in building controls are crucial to occupant comfort and achieving energy efficiency. The calculation of mean radiant temperature using an IR camera in real-time and incorporating thermal comfort parameters as a building control is unique to this project. The process shown in Figure 2.1 is a combination of different methods, each working independently as a separate block towards sending a comfort signal to the thermostat. The input variables to each independent block in Figure 2.1 were entered

manually. In the first step, IR images were captured with validated camera viewing angles and measurement parameters. The next step was to section the room surfaces and extract surface temperatures using FLIR tools. The averaged radiometric results are used to calculate mean radiant temperature in Excel using geometrical correlation factors of an occupant with surrounding surfaces. The mean radiant temperature value along with other assumed and measured thermal comfort parameters were provided as inputs to an Excel comfort calculator (based on ASHRAE-55) to obtain the Predicted Mean Vote (PMV). The PMV is then translated into a BACnet signal as a thermostat setpoint to condition the space. The PMV served as the control variable in this present study to quantify thermal comfort and energy savings. The following figures and paragraphs describe the test room and apparatus we used in our methodology in detail.

2.2 The Test Chamber

Figure 2.2 shows the test chamber of the University of Idaho's, Integrated Design Lab (IDL) modeled in SketchUp. The IDL is located in Boise, Idaho. The location is designated under climate zone-5B as per ASHRAE 169-2006 standards. The IDL's test chamber consists of two rooms that are identical to each other.

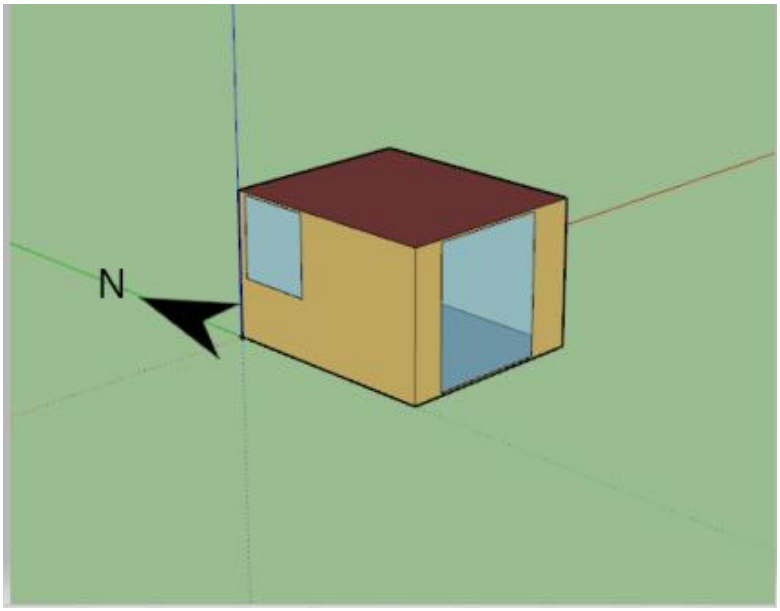

Figure 2.2: Test chamber modelled in SketchUp

The test chamber had an area of 109 square feet and consisted of two windows which are located on the south and west walls. The south and west walls are exposed to the outdoors. The east and north walls are interior walls attached to adjacent rooms. The window to wall ratio of the south wall was 60% and for the west wall was 19%. The south window was exposed to solar radiation and had adjustable blinds. The room was set up like a typical office environment. The floor is carpeted, and the ceiling has dropped acoustic tiles. The test chamber also has an overhead LED light fixture and a ductless

mini-split heat pump for space conditioning. Figure 2.3 shows images of the test chambers where we tested our methodology.

Figure 2.3: IDL Test Chambers

The MRT calculation was calculated in relation to the person in the room. The calculation requires the occupant's position in the room and geometrical correlation of the person with the surrounding surfaces. A baseline scenario was used to test and validate our methods for MRT and PMV calculation. The baseline scenario included an occupant seated in the room facing towards the east wall. The origin of the room was taken at the southeast corner. The coordinates of the occupant's position in the X-Y plane were 0.91 meters (2.98 feet) from the east wall and 1 meter (3.28 feet) from the south wall.

Figure 2.4: Baseline scenario captured by an IR camera

Figure 2.4 shows the baseline scenario used to validate our calculation for MRT and PMV values. In the baseline scenario, the occupant was seated and assumed normal working conditions. The occupant faced the east wall and was close to the south window.

The blinds were partially closed to avoid direct sunlight. The heat pump was set to heating mode with setpoint temperature at 71°F (21.6 ℃) and the measured air temperature was 67°F (19.6 ℃).

2.3 Understanding the IR Camera

Infrared thermography is a non-invasive technique that measures radiation emitted from bodies in the thermal band (7 – 14 μm) of the electromagnetic spectrum. The array of sensors in an IR camera does this by converting thermal radiation into temperature values. Each pixel in the resulting image is a temperature value calculated by Stefan Boltzmann law, with certain known influencing factors in advance (Garrido, Lagüela, & Arias, 2018). According to the wavelengths, the electromagnetic spectrum is divided into several regions. This ranges from 0.4 μm - 1000 μm lies in the infrared region. However much of the infrared range in the spectrum is not useful as it is blocked by the atmosphere (Ruben, et al., 2014). The useful portions for thermographic applications are mid-wavelength infrared (MWIR) that ranges from 3 μm - 5 μm and thermal infrared (TIR) that ranges from 7 μm - 14 μm. MWIR devices are commonly used in high-temperature sensing applications and TIR is used for sensing ambient temperatures (Laguela, Diaz-Vilarino, & Roca, 2016).

The calculation of mean radiant temperature involves surface temperature readings and geometrical correlations of the person and surrounding surfaces. The most common practice is to have thermocouples as a standard for measuring indoor surface temperatures (Porras-Amores, Mazarron, & Canas, 2013). However, it is complicated and impractical to measure and consistently feed a control loop using thermocouples in real-

time. For example, for the calculation of MRT indoors, surface temperatures of all the surrounding surfaces are needed. This would require at least 6 thermocouples attached to wall surfaces and some on window surfaces depending on the room geometry. The wiring of sensors to the main control loop and point measuring technique makes it complicated for MRT calculation. Infrared cameras are a non-contact surface temperature measurement device, that can cover wide spatial areas as compared to a single sensor temperature output. Depending on the IR resolution, a single IR frame could contain radiometric data for two or three surfaces. This is ideal for generating MRT values in a space with respect to an occupant which is the approach in this study.

For accurate surface temperature measurements from an IR camera, a proper understanding of the radiometric properties of the surrounding environment is required (Fokaides, Jurelionis, Gagyte, & Kalogirou, 2016). Non-contact temperature sensing depends on precisely addressing surface temperature characteristics, atmospheric interference, and the imaging system. Emissivity, reflectivity, and distance are characteristics that influence IR surface temperature measurements. The spatial resolution from an IR camera is the function of image focus, blur, and pixel resolution. The viewing angle from an IR camera is important for measuring accurate surface temperature readings. Straight viewing angles should be avoided when measuring surfaces that have low emissivity and high reflectivity such as a window in a room. In such situations, view angles less than 60° normal to the surface are recommended to avoid impact from reflections. The suggested emissivity value set should be ideally greater than 0.90 to reduce the effect of background temperature reflections and glares (FLIR, 2016). For this study, we used a FLIR C2 infrared camera from FLIR systems. The camera retails for

$499. We chose this camera because of its relatively price and features such as integration with FLIR tools and the ability to connect to a computer via USB.

Table 2.1: FLIR C2 specifications

Specification	**FLIR C2**
USB	2
Operating temperature range	-10°C to +50°C
Color palettes	Iron, Rainbow, Gray
Digital camera	3.07MP
NETD, Thermal sensitivity	100mk, <0.10°C
Field of view	41° x 31°
IR resolution	320*240
Focus	Focus free
Frame rate	9hz
Minimum focus distance	Thermal, 0.15m (0.49ft)

Table 2.1 lists the specifications of the FLIR C2 infrared camera. It captures a temperature grid with a resolution of 320 x 240 pixels. Higher resolutions can cover a larger frame in space whereas, with lower resolutions more images are needed to cover the same area. The focus option on the FLIR C2 is not available. The IR camera performs a non-uniformity correction (NUC) at timed intervals. NUC is an image correction carried out when the output image becomes spatially noisy. It was noted that during camera start-ups the NUC corrections happen more often at the beginning of the operation and decreased over time. The user does not have control over the NUC corrections. The FLIR C2 is also equipped with a digital camera of 3.7-megapixel

resolution. Multi-Spectral Dynamic Imaging (MSX) is a feature in FLIR C2, that enhances the clarity of the thermal images by combining visual images with infrared images in real-time. The MSX feature in the FLIR C2 is a great feature for improved clarity of the IR images. In terms of temperature accuracy, the industry standard of IR camera measurement is +/- 2°C (+3.6°F).

2.4 Surface Temperature Measurement Validations of an IR camera

Understanding the measurement techniques of the IR camera is important for obtaining reliable surface temperature readings indoors. The findings from our comparison test apparatus allowed us to use the IR camera with better clarity. The measurement accuracy of an IR camera is important in MRT calculation. Thermocouple surface temperature measurements were taken as a reference in our study to validate the surface temperature readings measured from the FLIR C2 infrared camera. The three measurement parameters settings in the infrared camera are emissivity, reflectivity, and distance. At first, without the proper set values of measurement parameters of the IR camera, the surface temperature measurements deviated highly from the thermocouple temperature values. An accurate surface temperature reading from an IR camera is the result of proper settings of the measurement parameters (FLIR, 2016). Emissivity is the measure of a surface's efficiency emitting thermal energy with reference to a perfect blackbody. Mikron has documented emissivity values of various surfaces at a given temperature for infrared thermometry which can be referred to as an initial setting parameter in infrared studies (Mikron Instrument Company). Most of the building materials have high emittance. Surfaces will appear colder if proper emissivity values are not set in the measurement process.

Table 2.2: Emissivity values of common materials (FLIR, 2016)

Material Description	Emissivity
Asphalt	0.90 - 0.98
Concrete	0.92
Wood	0.9
Water	0.92 - 0.96
Ice	0.96 - 0.98
Brick	0.93 - 0.96
Lacquer, paint	0.80 - 0.95
Lacquer, flat black	0.97
Textiles	0.90
Skin, human	0.98
Aluminum, polished	0.04 - 0.06
Aluminum, anodized	0.55
Steel, rusty	0.69
Steel, stainless	0.16 - 0.45

Table 2.2 shows the emissivity values of common materials found in buildings. The emissivity setting in the IR camera was set at 0.95 which is an approximation as most building materials have high emittance. Reflectivity was set to measured air temperature near the camera. The air temperature was measured using a Hobo U12 data logger placed near the IR camera. The distance parameter in the IR camera from the measured target did not have much significance with the radiometric data obtained in the IR camera but is correlated to the IR image's clarity and sharpness. The distance parameter was set to zero in our study for indoor surface temperature measurements.

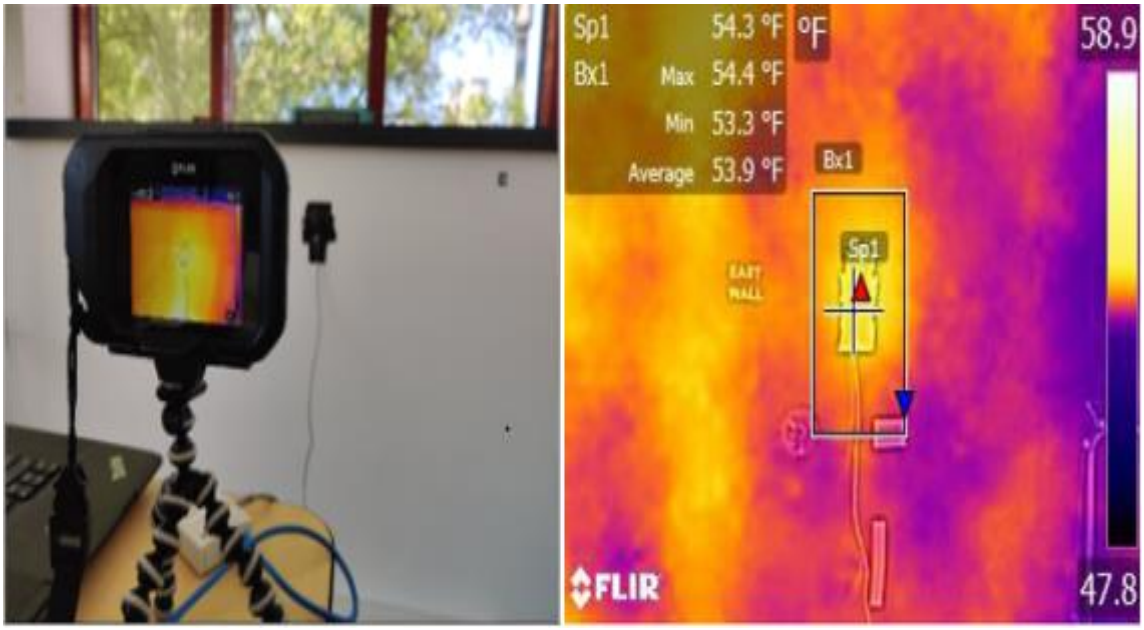

Figure 2.5: IR camera measuring surface temperature at thermocouple location

Figure 2.5 shows the IR camera focused on the thermocouple location for surface temperature measurements. The data logger used for recording the thermocouple surface temperature was Hobo U12 Temp/RH/2 external Datalogger (Part #U12-013). The logger has an air temperature and humidity sensors in-built and channels to connect external sensors. The external thermocouple used for our validation study was the Hobo temperature sensor, TMC6-HD. The 12- bit surface temperature sensors were placed against the wall with a layer of 5 mm insulation tape and a second layer of duct tape over the insulation tape. The tapes were attached tightly over the insulation tape and ensured no air gaps. This is was done to ensure the thermocouple sensor was tightly placed against the wall so it would read accurate surface temperatures and not air temperatures. For the comparison test, the thermocouples attached to the walls were measured with an IR camera at approximately 90° and the thermocouples attached to the windows were measured at approximately 60°.

The image on the right in Figure 2.5 shows IR image analysis performed in FLIR tools to acquire surface temperature from FLIR C2 at the thermocouple location. The red and blue triangles in the box plot show the maximum and minimum temperatures in the box. The average temperature of the box and spot temperature can be read from FLIR tools. We used spot, line and box features in FLIR tools to relate the IR camera's surface temperature and recorded thermocouple temperature.

Figure 2.6: IR camera mounted on a tripod

Figure 2.6 shows an IR camera mounted on a tripod in the IDL chamber and focused on the east wall for image acquisition. The IR camera was mounted on a tripod and was approximately 60 inches from the floor similar to a conventional thermostat placement on a wall. For surface temperature readings from the ceiling and floor, the IR camera was manually rotated to capture the IR image. Camera mounts used strategically can improve the camera stability, image focus, and reduce jitter of the camera (FLIR, 2016).

In our comparison study, multiple thermocouples were attached to the surrounding room surfaces. The comparison study was performed to understand the measured surface temperature deviation of the IR camera with the thermocouple temperature readings. Nine readings were recorded for ceiling, floor, north wall, south window frame and west wall at a one-hour interval between 9:00 am to 5:00 pm. For the south window, only 3 readings of the measured values were used in this study, and for the west window, 8 readings were used. The comparison results are presented in the results section.

2.5 Surface Temperature Extraction using FLIR Tools

FLIR tools is a free software solution from FLIR systems to primarily analyze, import, and edit captured images from the FLIR camera. It is a user-friendly software and a simple tool to analyze and section the IR image. It also has the capability to export an IR image as pixel data into a CSV or spreadsheet. MRT calculation involves geometrical correlations between the person in space to the surrounding's surface temperatures. The surrounding surfaces that were used in MRT calculation included east wall, west wall, south wall, north wall, floor, ceiling, south and west windows. With known measurement parameter settings, the surrounding surface temperatures were captured manually from the IR camera. The acquired images from the IR camera were analyzed using FLIR tools.

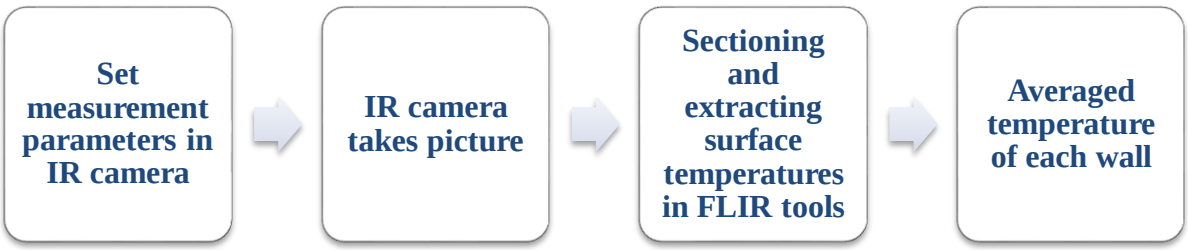

Figure 2.7: Process to obtain the surface temperature of the section understudy

Figure 2.7 shows the process we followed to obtain temperatures of surfaces understudy. FLIR tools were used to import, analyze, and extract the radiometric values from the IR camera for the average temperature value of each wall. When extracting temperatures, sectioning of surfaces understudy was analyzed using the FLIR tool's box plot feature. As the name suggests, the feature enables the user to draw a box plot on the region of interest in the IR image to obtain the averaged radiometric value.

As the walls of the room are not iso-thermal, we manually divide each wall into small sections and average the temperatures of small sectioned surfaces which are essentially iso-thermal. The sectioned surfaces are assumed to be grey (i.e. emittance is equal to absorptance) and the radiation emitted and reflected follows Lambert's cosine law (Fanger, 1970). As MRT is calculated in relation to the occupant in space, the occupant is excluded from the sections. All other objects in space are included with the reference wall surface temperature measurement. Walls that included windows were sectioned separately, differentiating the wall and window surface temperatures. Typically, a wall was divided into two or three smaller sections depending upon spatial resolution from the acquired IR image as most frames contained more than one wall. The final surface temperature for the wall or window was calculated as the averaged sum of

all the divided sections. This method of sectioning using box plots in FLIR tools is shown in Figure 2.8.

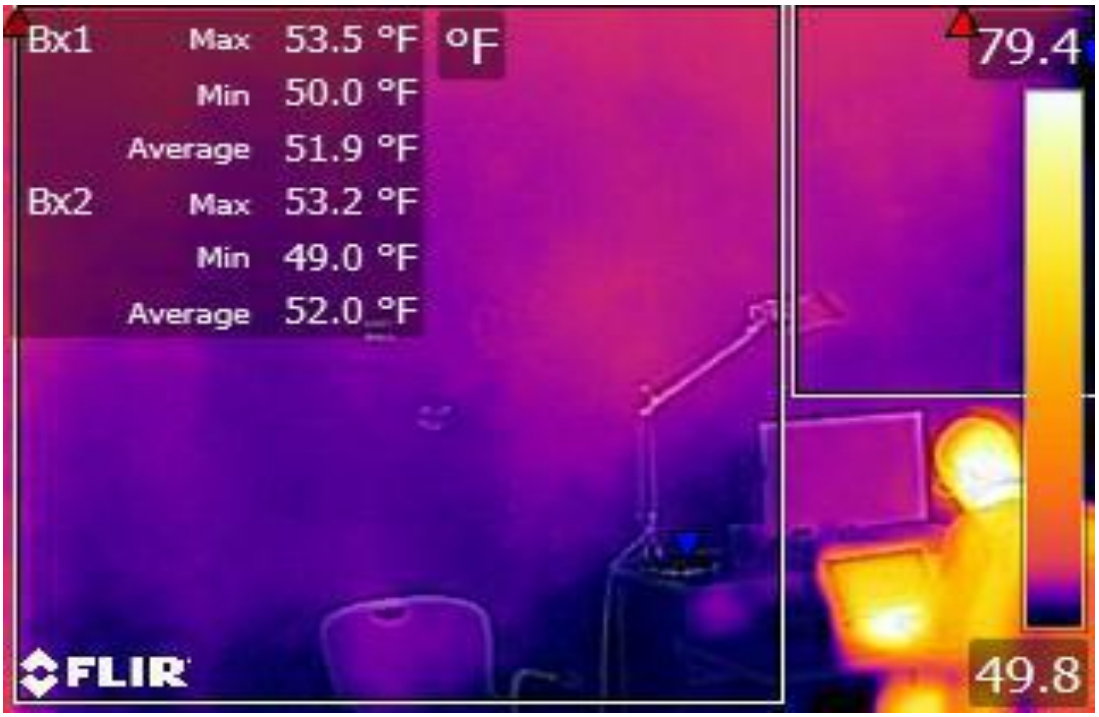

Figure 2.8: Sectioning performed using FLIR tools

The same method is repeated for surface temperature extraction from surrounding room surfaces and used for MRT calculation.

2.6 Mean Radiant Temperature

"Since the mean radiant temperature has a considerable influence on man's heat loss and thus on his state of comfort, its calculation is important in the detailed thermal analysis of a room" (Fanger, 1970). The MRT in relation to an occupant in space is of interest when considering space conditioning. MRT values differ for a person standing to that of a person seated and changes with a person's location and orientation in the room. In low-temperature radiation, the absorptance is equal to the emittance and the emittance

of the person has no influence on MRT. But in calculation with room surroundings, appropriate emittance value must be considered. In rooms with uniform wall surface temperatures, the emittance will have no influence on the MRT. In rooms with non-uniform surface temperatures, emittance from the surfaces will have a relative influence on the MRT. View factors need to be known for the calculation of MRT in relation to surroundings.

MRT means if surfaces are cooler than skin temperature, energy will be drawn away from the body by radiation resulting in cooling sensation. Similarly, if surfaces are warmer than skin temperature, the release of energy from the body will be hindered via radiation resulting in a sensation of heat (Bean, 2013). For better accuracy in the calculation of MRT, the view factor that describes geometrical relationships between occupants and surfaces needs to be applied. Considering a rectangular room, the calculation must consider all six sides of the room, surfaces above and below the center of gravity, and all with reference to the coordinate position of the occupant in the room. The closer the occupant is to a surface, the greater is the thermal influence felt by the occupant. For example, a person sitting near to a cold window will feel discomfort as compared to other occupants in a room (Halawa, Hoof, & Soebarto, 2014). Hence, MRT incorporation in building controls is critical to the evaluation of the accurate thermal comfort needs of occupants indoors. It is calculated as the average value of the surrounding temperatures and weighted according to the corresponding view factors.

2.6.1 View Factors

When considering radiative heat exchange between two or more surfaces, energy exchange depends on surface geometries, orientations, radiative properties, and temperatures. To calculate radiative heat exchange between two surfaces, view factors are used and are also known as angle factors, configuration factors, or shape factors (Incropera, Dewitt, Bergman, & Lavine, 2007).

In the present study to calculate MRT using infrared cameras, view factor relations between the surfaces of the room and person is considered. In this study, the method of calculating MRT is based on the classical approach developed by Fanger and correlated view factor equations from Representatives of European Heating and Ventilation Association (REHVA) guidebook (REHVA, 2009). The below paragraphs describe the equations and approach we used to divide the test chambers into rectangles for the calculations of view factors from Fanger's approach.

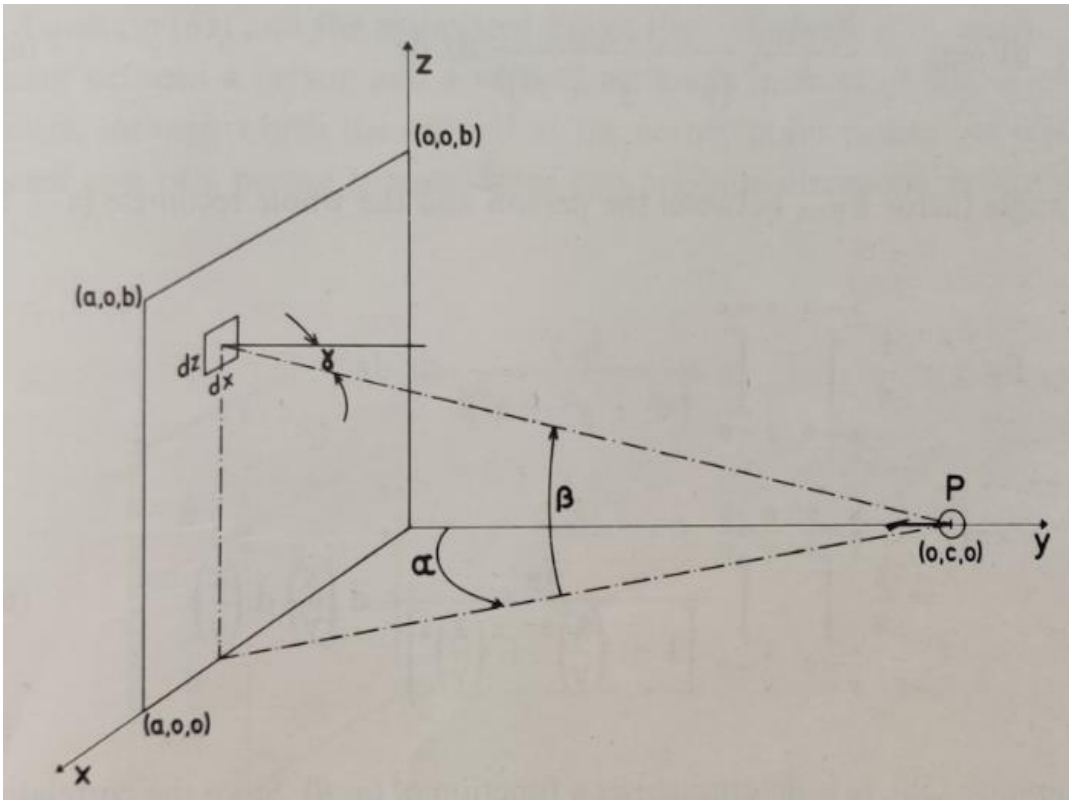

Figure 2.9: Diagram for evaluation of view factor between a person and rectangle (Fanger, 1970)

Figure 2.9 shows a diagram used for view factor evaluation between a person and a rectangle. The rectangle (a x b) is in the X-Z plane. The person's location in the orthogonal coordinate system is (0, c, 0) denoted as P. A typical room is enclosed, rectangle in form, and surrounding surfaces include walls, floors, ceiling, and windows.

Therefore, in the calculation of MRT, view factors between the person and horizontal and vertical rectangles of the room are of primary interest. As shown in Figure 2.9 for a person located in the orthogonal coordinate system, the distance from the person to the system is c and dimensions of the system are a and b. The view factor between the person and the whole rectangle (a x b) in the X-Z plane can be determined by numerical integration. As the orientation of a person in a room often changes, relations that are

derived for when a person's location is known, and orientation unknown is used in this study. F_{P-A} represents the mean view factor between the person and a rectangle when a person rotates around a vertical axis. This view factor as obtained from numerical integration can be written as,

$$F_{P-A} = \frac{1}{\pi}\int_{\frac{x}{y}=0}^{\frac{x}{y}=a/c}\int_{\frac{z}{y}=0}^{\frac{z}{y}=b/c}\int_{\alpha=0}^{\alpha=2\pi}\frac{f_p}{\left[1+\left(\frac{x}{y}\right)^2+\left(\frac{z}{y}\right)^2\right]^{3/2}}$$

where F_{P-A} is the view factor between the person and the whole rectangle (a x b) and f_p is determined as a function of α and β.

$$\alpha = \tan^{-1}\left(\frac{x}{y}\right)$$

$$\beta = \tan^{-1}\frac{\frac{z}{y}}{\sqrt{\left(\frac{x}{y}\right)^2+1}}$$

Fanger describes the method of dividing the surfaces of the room into rectangles for calculating view factors using dimensional parameters (Fanger, 1970). Using simple angle factor algebra diagram as shown in angle factors can be determined for rectangles of any size with the normal at the corner and passing through the center of the person using simple angle factor algebra for the person and rectangle A. The angle factor algebra equation is,

$$F_{P-A} = F_{P-ABCD} - F_{P-BC} - F_{P-CD} + F_{P-C}$$

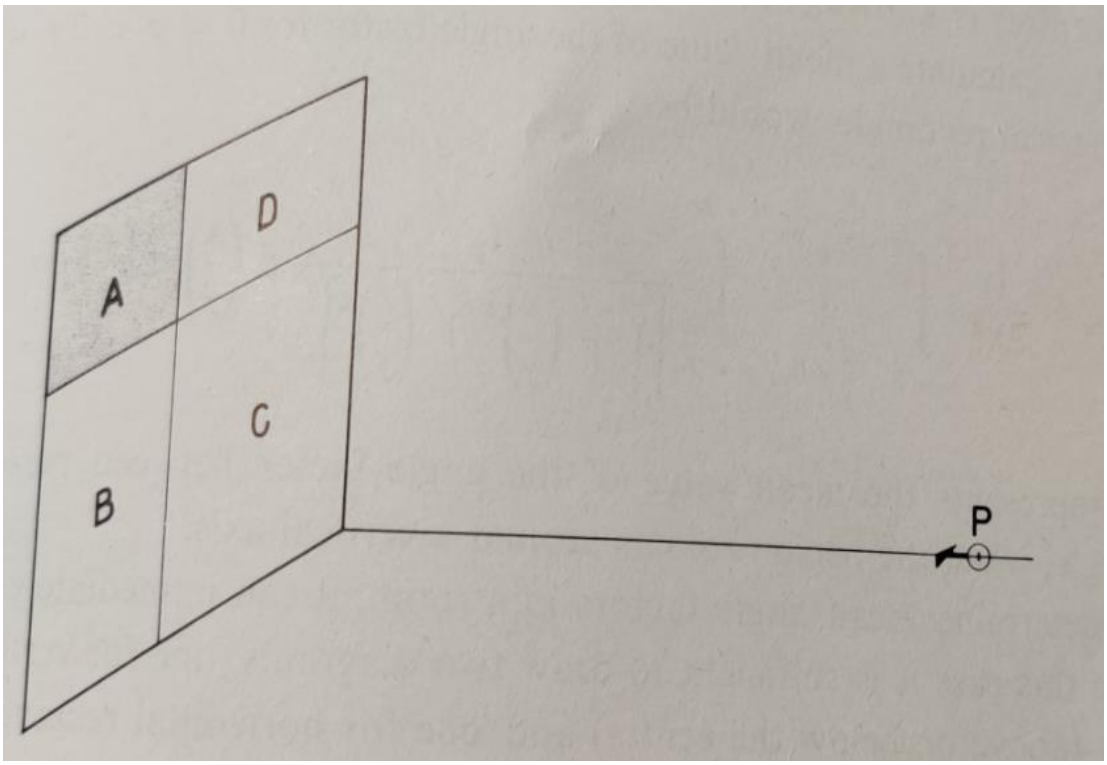

Figure 2.10: Angle factor algebra (Fanger, 1970)

The view factors at the right of the algebraic equation can be determined from Figure 2.10 using corresponding a/c and b/c values. View factors are dimensionless and are a function of a/c and b/c values, a and b are the dimensions of the rectangle and c is the distance between the occupant in space to the referred rectangle. The projected area factors will be the same for the front and back of the person and the same diagram can be used if windows or heating/cooling panels are not present (Fanger, 1970).

In a similar manner, the room under our present study (IDL test chambers) was divided to further calculate view factor relations between the person and the surrounding surfaces as shown in Figure 2.11.

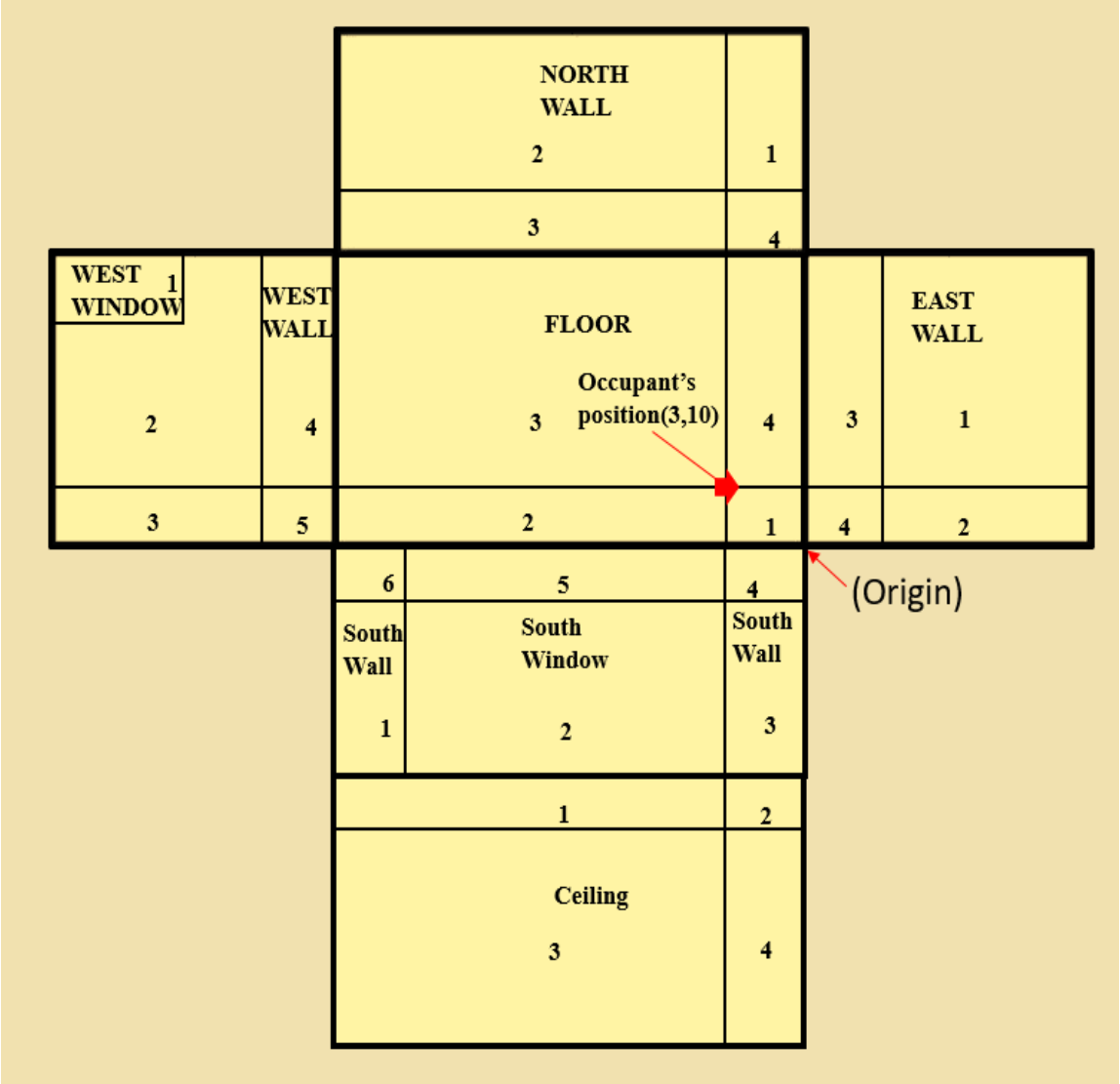

Figure 2.11: IDL room geometry divided for view factor calculations

Figure 2.11 shows the IDL room geometry divided for view factor calculations in accordance with the angle factor algebra diagram. With the occupant's known position in the room, the surrounding surfaces (east wall, west wall, north wall, south wall, floor, and ceiling) in relation to the person are divided into six rectangles. The occupant position is marked by the red arrow at (3,10) meters. The IDL room geometry was divided into 27 rectangular sections for view factor correlation with relation to the occupant's position. In

all the cases, normal to the corner point of the rectangle passes through the center of the person. The view factor from above and below the occupant's center vary by about 30% due to the asymmetry of the human form. As our method is focused on obtaining mean radiant temperature in space for the occupant's in a seated position, 0.6 m is used in our calculations corresponding to the normal height of the center of mass for an occupant in a seated position.

P. O Fanger developed a large set of graphs for the evaluation of view factors for rectangular surfaces, but using visual interpretations of these graphs can lead to reading errors (G.Cannistraro, G.Franzitta, C.Giaconia, & G.Rizzo, 1992). As Fanger's numerical integration approach is difficult to compute in Excel, we used Dunkle's approach to calculate view factors (Howell, 2010) (Dunkle, 1963). The results of this method deviate up to 27% from Fanger's results and involve errors up to 20% as Dunkle approximated the human body to a sphere for his calculations (Fanger, 1970). As the view factor relations calculated in Excel using Dunkle's method led to view factor summations significantly greater than unity, we proceeded with the view factor equations found in the REHVA guidebook (REHVA, 2009).

2.6.2 REHVA Equations

The REHVA equations required simple algebra calculations and were cited or used in an ASHRAE research project-1383 (Bean, 2011). The REHVA guide follows Fanger's approach to calculate angle factors but approximates the numerical integrations into algebraic expressions for ease of calculation.

Table 2.3: Equations for calculations of angle factors (REHVA, 2009)

	F_{max}	A	B	C	D	E
Seated Person, Vertical Surfaces: Wall, Window	0.118	1.216	0.169	0.717	0.087	0.052
Seated Person, Horizontal Surfaces: Wall, Window	0.116	1.396	0.13	0.951	0.08	0.055

Table 2.3 shows the value of the constants used for angle factor calculations as mentioned in the REHVA guidebook. The below-mentioned equations were used to calculate view factors in relation to an occupant in space.

$$F_{p-N} = F_{max}\left(1 - e^{-(a/c)/\tau}\right).\left(1 - e^{-(h/c)/\gamma}\right)$$

$$\tau = A + B(a/c)$$

$$\gamma = C + D(b/c) + E(a/c)$$

where F_{max}, A, B, C, D, and E are constants referred from Table 2.3 for the calculation of view factor relations for a seated occupant, and a/c and b/c are lengths of the rectangles. The view factor relations with the correlated surface temperatures measurements from the IR camera are used to calculate MRT.

2.6.3 MRT Tool

The MRT tool is a spreadsheet developed in Excel to compute MRT with relation to an occupant at any point in space. Two-dimensional coordinate translations of the room were correlated with REVHA view factor equations. For a seated person, his center of mass is only 0.6 meters from the floor while the center to ceiling is 1.8 to 2 meters.

Hence, the floor has the highest angle factor of all surfaces with relation to the occupant (REHVA, 2009).

The X and Y position of the occupant in the room is required to compute the view factor relations for estimating the MRT. The position of the occupant in the baseline scenario were inputs in the MRT calculator. The baseline model is with reference to the southeast wall as the origin. With X and Y known positions, each room surfaces were divided into rectangles for the calculation of a/c and b/c values above and below the center of gravity of the person. Each wall section was divided into four smaller rectangular sections with reference to the occupant in space as shown in Figure 2.11. For walls with windows, the division of rectangles will differ depending on the person's location. The a/c and b/c values in Excel were calculated by two-dimensional coordinate translations linked to the X and Y coordinate inputs of the person seated in the room. The method in Excel was automated and could calculate MRT values at any point in the room. The Excel spreadsheet developed was specific to IDL's test room geometry. The method could be applied to any room geometries to calculate MRT by updating the geometry inputs. Once surface temperatures of the space retrieved from the IR camera and correlated view factors are known, these values were used to calculate MRT. The equation to calculate MRT is derived from surface temperatures, radiative properties, and correlated view factors. The relations are explained below.

The extent to which radiant energy flows away from a surface is called radiosity, B. The MRT value can be determined in an enclosure having N surfaces of temperature $T_1, T_2 \ldots T_N$. The first term in the radiosity equation denotes emitted surface radiation and the second term denotes reflected radiation.

$$B = \in \sigma T^4 + \rho H$$

where ρ is the reflectance, $\in$ is emittance, H is incident energy arriving at the surface and, σ is the Stefan-Boltzmann constant. From the definition of mean radiant temperature and upon applying radiosity values, the relation is obtained as:

$$\varepsilon_p \sigma (T_r^4 - T_{cl}^4) = \varepsilon_p \sum_{i=1}^{N} B_i \, F_{P-A_i} - \varepsilon_p \sigma T_{cl}^4$$

where ε_p is the emittance from the person, F_{P-A_i} is the view factor between the person and the surface i and T_{cl} is the person's surface temperature. As most building materials have high emittance and reflections are often disregarded as approximations, we can write the MRT equation that was used as (Kalmar & Kalmar, 2012):

$$T_r^4 = \sum_{i=1}^{N} T_i^4 \, F_{P-A_i}$$

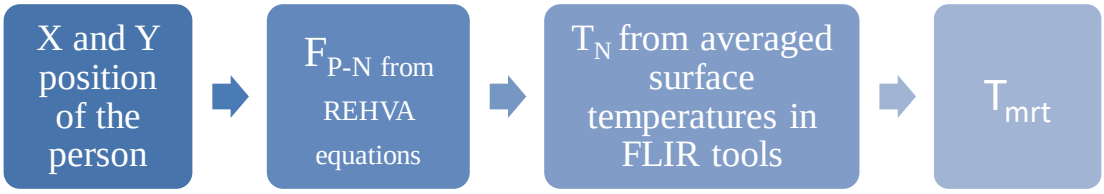

Figure 2.12: Block diagram for calculating MRT in Excel

Figure 2.12 shows the block diagram for calculating MRT in the tool developed in Excel. The known X and Y position of the person in the room is manually entered in the Excel MRT tool. The MRT tool calculates the view factors with respect to the occupant position with all the surrounding surfaces using REHVA equations. The acquired surface

temperatures from the IR camera are averaged using FLIR tools and are inputs to the MRT tool. The MRT equation calculates the MRT value for the preferred position in the room and is linked to the PMV tool to obtain the PMV value. The results and verification of this approach are presented in the results section.

MRT is one of the most important parameters governing human thermal comfort. But the control variable that drives HVAC systems for an artificially controlled space should just not be dependent on the MRT value. There are five additional parameters that govern thermal comfort in occupants from Fanger's approach. This is discussed in the next paragraphs. We use this combined value of all the parameters to determine the indoor temperature that can be used to drive HVAC systems such as the systems that are human-centric and efficient in operation.

2.7 ASHRAE Standard-55: Thermal conditions for human occupancy

The American society of heating, refrigeration, and air-conditioning engineers, (ASHRAE) standard 55 is titled "Thermal conditions for human occupancy". This standard was first created in 1966 and its present edition is ASHRAE 55-2017. We used the computer program mentioned in the normative appendix B of the ASHRAE standard 2013 for the calculation of PMV-PPD which is the basis for comfort control logic in this study translated into an Excel spreadsheet (ANSI/ASHRAE, 2013). The standard recommends a PMV in the range of ± 0.5 and PPD < 10% considered acceptable comfort standards in occupancy conditions. The ASHRAE standard-55 shows a graphic comfort zone method and analytical comfort zone method for determining comfort operative temperatures indoors. Both the methods assume MRT equal to the convective air

temperature under certain conditions which leads to misinterpretation of the occupant comfort of in space.

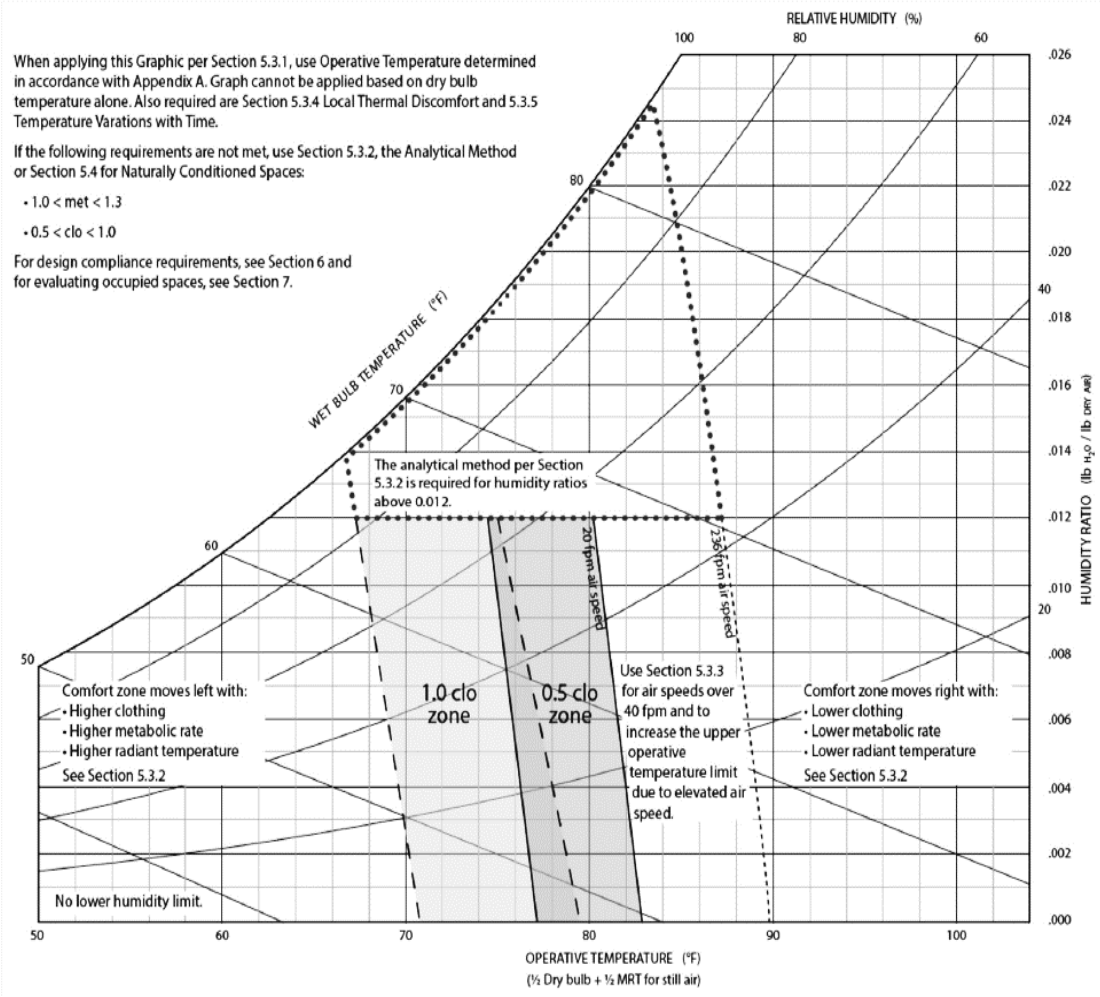

Figure 2.13: Acceptable ranges of operative temperature and humidity in IP units (ANSI/ASHRAE, 2013)

Figure 2.13 shows the graphic comfort zone method for acceptable ranges of operative temperature and humidity for at least 80% of occupants involved in light sedentary activities, assuming typical summer and winter clothing levels. The ranges are valid for mean airspeed <=0.15 m/s (30 ft/min), and for occupants who are in space for

more than 3 hours or more. It represents to occupants with metabolic rates between 1.0 and 1.3 met and clothing value between 0.5 and 1.0 clo. This is an ideal condition for standard office settings. The above ranges shown in Figure 2.13 of operative temperatures can be inappropriate and misleading to the audience if used as a parameter for operative temperature. It depicts that mean radiant temperature is equal to air temperature which is a flaw in practice and design. “It is inappropriate because the operative temperature is not a property of a mixture of air and water vapor which can be located on a psychrometric chart” (Halawa, Hoof, & Soebarto, 2014). Any condition in which the MRT is not equal to the air temperature can hardly be identified on the chart (Halawa, Hoof, & Soebarto, 2014).

Due to the thermal interaction between the building envelope, occupancy, weather conditions and the HVAC systems, an ideal steady-state condition in practice is rarely achieved indoors (Hensen, 1990). Conventional thermostat setpoints seek to achieve constant indoor air temperatures. However, the temperatures indoors may vary by 3 to 4 degrees indoors during HVAC usage and is not uniform (Metzger & Norton, 2014). Hence studies and practices assuming the determination of operative temperature under steady-state conditions are potentially flawed. MRT is one of the most important parameters in the evaluation of the human physiological and psychological perception of the thermal environment along with other governing factors (Kántor & Unger, 2011). Hence the emphasis on the measurement of accurate MRT indoors is important in comfort controls in buildings and is the primary focus in this study.

2.7.1 PMV Tool

The PMV tool was a spreadsheet developed in Excel based on the ASHRAE standard. The PMV algorithms in Excel consists of five parts to calculate the PMV-PPD value. The algorithms of each section are used consecutively in the next parts for calculations. The first section is the user-defined inputs. The six user inputs include air temperature, mean radiant temperature, relative humidity, clothing, metabolic rate, and air velocity. The metabolic rate of 1.1 was used in this study as per the baseline scenario with occupant seated and typing. A clo value of 1 was used based on the occupant's clothing insulation resembling winter wear. The air temperature was measured using a Hobo U12-012 data logger and was measured in the test chamber to be 19.6°C. In this study, the focus was to develop a simple tool to calculate MRT indoors using current technologies to acquire radiometric data. The method was developed with the combination of acquired radiometric images from an IR camera that was validated with thermocouples and occupant based MRT calculation from the REHVA guidebook. The developed tool in Excel for determining MRT and was linked to the PMV -PPD spreadsheet for obtaining a comfort control signal. The value assumed for typical indoor conditions was 0.1 m/s and relative humidity was measured from a Hobo U12-012 data logger in the test chamber and found to be 34%.

The second section is an algorithm to convert the inputs into SI units. The third section calculates the impact that convection has on a person's clothing, which is to consider the effects of natural and forced convection. In this part, a series of iterations are carried out by the code until the difference between forced and natural convection temperature estimations differ by less than 0.00015. The fourth section calculates the heat

loss components, which are heat loss through skin, heat loss by sweating, latent respiration, dry respiration and heat loss by radiation and convection. The fifth section consists of the final PMV and PPD calculations. The PMV-PPD calculations were computed for the baseline scenario and are discussed in the results section.

2.7.2 Translating PMV and Occupancy data into a Building Control Signal

The purpose of using an IR camera in building controls is to send occupant centered heating and cooling signals to the HVAC system. The established protocol for sending control signals is the Building Automated Control Network Protocol or BACnet. Building Automation and Control Network (BACnet) is a standard communication protocol developed by ASHRAE which has been used by the American National Standards Institute (ANSI) and by International standard organization (ISO). BACnet was developed to allow building owners to use control equipment from different manufactures to achieve inter-operability. BACnet uses an object-oriented method for identifying, organizing the data in a controller (Reddy, Kreider, Curtiss, & Rabl, 2017). However, BACnet does not provide control, only protocols for communication. It supports building automation protocol in BACnet.

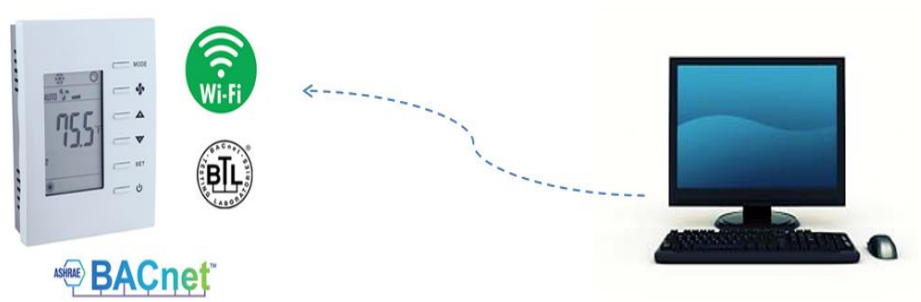

Figure 2.14: Comfort signal communicated wirelessly from computer to thermostat

Figure 2.14 shows the PMV value we obtained communicated wirelessly to the BACnet thermostat. Our aim was to verify that the PMV value could be translated as a BACnet signal to a thermostat. We used BACnet embedded wireless thermostat, BAST-221C-BW2 BASstat from contemporary controls as our controller. This series of thermostats allows seamless integration into BACnet/IP networks using a Wi-Fi connection. A Wi-Fi enabled laptop can detect the thermostat as an access point. To further translate the computed PMV values, we used the BACnet discovery tool (BDT) to translate our value as a BACnet signal. BDT is an open-source software tool available from contemporary controls. It can be used to read and write object name property, object ID property, discover BACnet devices, read trend log objects, and perform various other functions. BDT establishes communication with the BASstat thermostat. Once the network is established, we can change the object properties as needed. The object properties in the thermostat include occupied/unoccupied conditions, heating/cooling modes, and several other options. Typically, a thermostat tries to maintain a certain air temperature keeping the room within a certain dead band between heating and cooling

setpoints. In the present study, the setpoints were manipulated to maintain certain comfort levels.

Table 2.4: PMV value translation

Occupancy condition	PMV value	Thermostat command
if occupied	**< -0.5**	heat
	0	off
	> +0.5	cool
if not occupied	**-3 to +3**	Value will float

Table 2.4 shows PMV value translations and command followed by the thermostat during occupied and unoccupied conditions. If during occupied conditions the PMV value generated drops below -0.5, then the setpoints are increased above the current air temperature to force the heating system on. Similarly, if the calculated PMV rises above +0.5, the thermostat is to call for cooling. During unoccupied times, the setpoints are expanded dramatically and the PMV is allowed to float anywhere between $\pm$3 as a setback condition. The results of the PMV comfort calculations and baseline scenarios are presented in the results section.

2.8 Energy and Comfort Analysis Using PMV Based Control in Buildings

Our research included a comparative simulation between the conventional thermostatic control and PMV based control is studied to investigate the dynamics of thermal comfort and energy consumption for a small office. The U.S Department of Energy (DOE) software program, EnergyPlus version 9.2.0 was utilized for this study.

Most U.S commercial buildings are small to medium-sized and accommodate the largest population of workers (U.S. Department of Energy Office of Energy Efficiency and Renewable, 2004). In this study, a small office prototype developed by Pacific Northwest National Laboratory (PNNL) was used as the reference to study differences in the controls. The building geometry and HVAC loads were obtained from the PNNL database of standard building types based on CBECS data and ASHRAE Standard 90.1 prototype building model (Winiarski, Jiang, & Halverson, 2006) (Winiarski, Halverson, & Jiang, 2007) (ANSI/ASHRAE/IES Standard 90.1, 2016). These prototype models are used by organizations to test the impacts of new energy codes. Within EnergyPlus, the small building prototype files were updated to 9.2.0 from the 8.0 version. In order to maintain consistency with traditional thermostat settings, the same building occupancy schedules, and HVAC system sizing was used for the PMV based control building model.

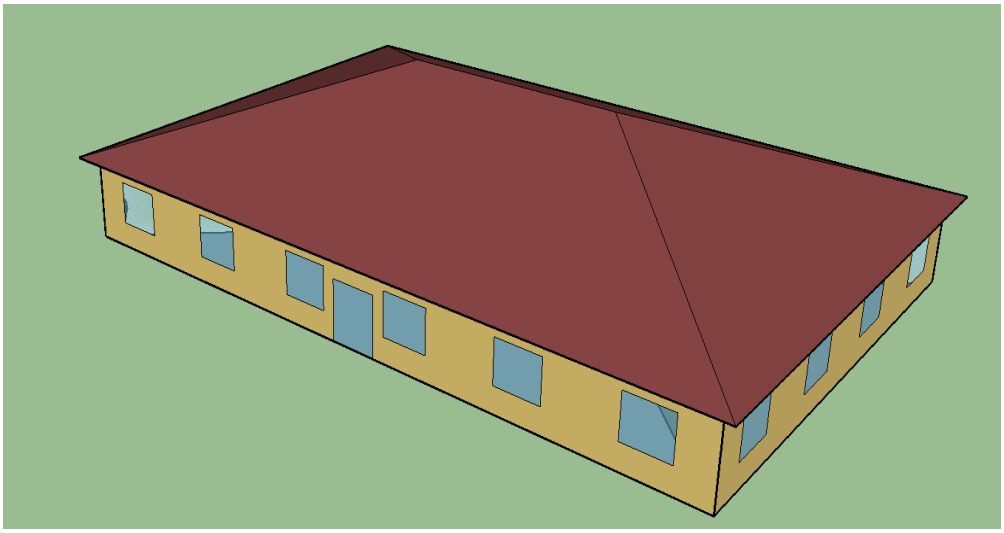

Figure 2.15: PNNL small office prototype (Dave Winiarski M. H., 2007)

Figure 2.15 shows PNNL small office prototype energy model we used for our analysis in Energy Plus. The prototype is a one storey small building with a total floor

area of 5500ft^2. The window to wall ratio was 24.4% for south and 19.8% for other orientations. The thermal zones included four perimeter zones, one core zone and one unconditioned attic zone. The model can be paired with different weather files to estimate utility costs in different locations. Typical metrological year version 3 (TMY3) weather files were used for the small building prototype to estimate thermal comfort and energy use.

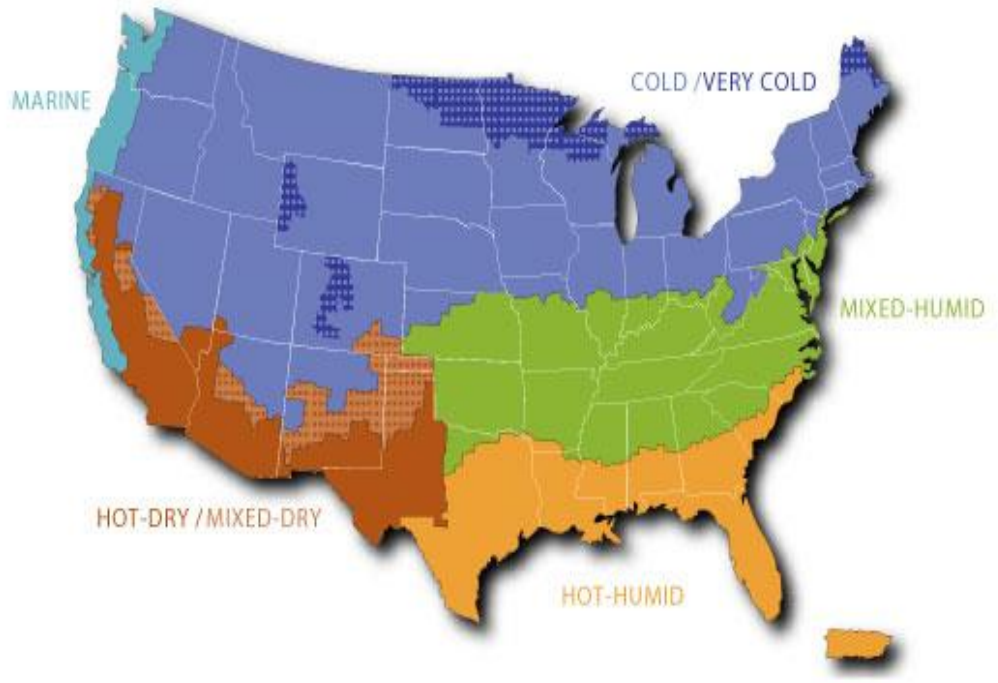

Figure 2.16: Building America Climate regions – CBECS 2012 (Baechler, Gilbride, Cole, Hefty, & Ruiz, 2015)

Figure 2.16 shows seven of the eight US climate zones in the continental United States. They are used by International Energy Conservation Code (IECC) and (ASHRAE) to partition the US into eight climate zones that account for minimum/maximum temperatures and humidity. The locations used in this study to compare the two control types included Zone 6B: Great Falls, Montana (cold, dry), Zone 2A: Tampa, Florida (hot,

humid) and Zone 4C: Seattle, Washington (mixed, marine) (169-2013, 2013). The HVAC system type assumed in the energy model was an air-source heat pump with the gas furnace as back-up heating. The distribution and terminal units were single zones, constant air volume air distribution, and one unit per occupied thermal zone. The systems are auto-sized to design day conditions. Initially, the small building prototype model was simulated with a conventional thermostat control type that uses standard air temperature setpoints and setbacks. The paragraphs and figures below discuss the schedules, setpoints, and setbacks the conventional air temperature control assumed in the energy model.

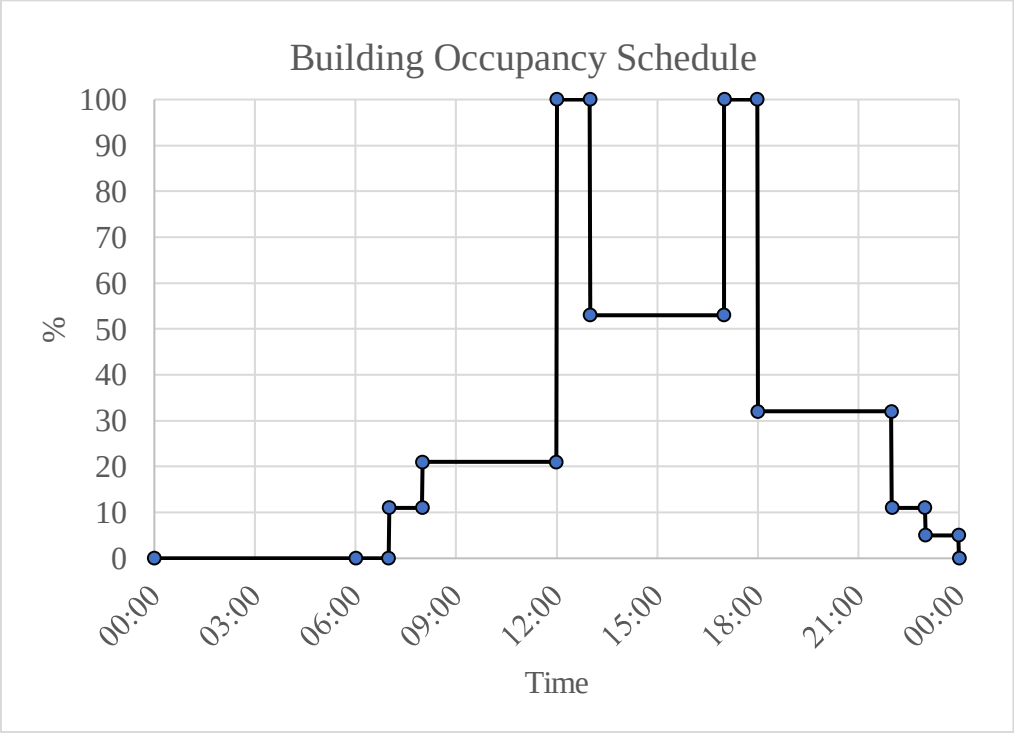

Figure 2.17: Building occupancy schedule

Figure 2.17 shows the default building occupancy schedule for small office buildings on weekdays. The building is unoccupied from 24:00 to 7:00 a.m. and occupied

from 7:00 a.m. to 10:00 p.m. at different capacities of people. For almost 2 hours in the working day, space is occupied at 100% capacity.

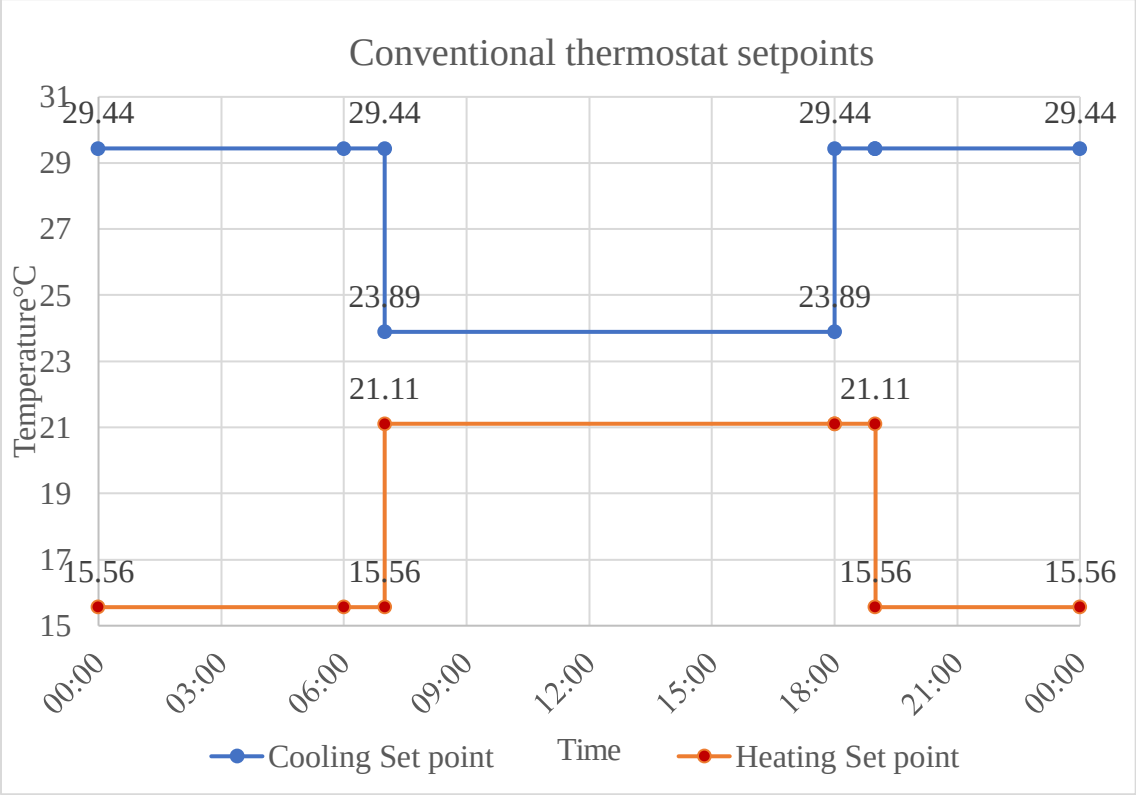

Figure 2.18: Cooling and heating setpoints followed by the conventional thermostat

Figure 2.18 shows the cooling and heating setpoints that the energy model assumed for the conventional thermostat in small office buildings. The cooling setpoint, represented by the blue line at maximum occupancy conditions (7 a.m. to 6 p.m.) is 23.89°C and the setback temperature is 29.44°C. The heating setpoint represented by the orange line, at maximum occupancy conditions (7 a.m. to 7 p.m.) is 21.11°C and the setback temperature is 15.56°C. The dead band between the heating and cooling setpoints was 2.78°C.

PMV control set-points

This section discusses the PMV control set-points used within EnergyPlus 9.2.0 for small building prototype. In the PMV control type model, the conventional thermostat control algorithms were changed to Fanger's thermal comfort model. EnergyPlus documentation was referred to alter the control code to Fanger's model (U.S. Department of Energy, 2019). Fanger's control type model included mean radiant calculations, work efficiency schedule, clothing schedule and air velocity schedules. The MRT was calculated using the zone averaged method and is an average point in the zone. "MRT is calculated based on an area-emissivity weighted average of all of the surfaces in the zone" (U.S. Department of Energy, 2019). In the model, the work efficiency schedule is set to zero. A value of zero in the model assumes energy produced in the body is converted to heat. The clothing schedules are divided into winter and summer months. For winter months the value is set to 1.0 corresponding to people wearing winter clothes and during summer months the value is set to 0.5 corresponding to summer wears. The air velocity schedule was set at default at 0.2 m/s year-round. The code for thermostat setpoints was adjusted within the model to have the thermostat trigger heating and cooling based on the PMV schedule instead of air temperatures. For the simulation study, two cases of PMV setpoints were analyzed based on optimum comfortable hours and energy-efficient conditions for all the site locations. The PMV thermostat schedules were set similar to the standard thermostat run for occupancy conditions in the building.

2.8.1: Case 1: PMV set point of ±0.5

A PMV setpoint of ± 0.5 is a standard PMV value indicating the optimum condition for thermally comfortable people in the occupied zone.

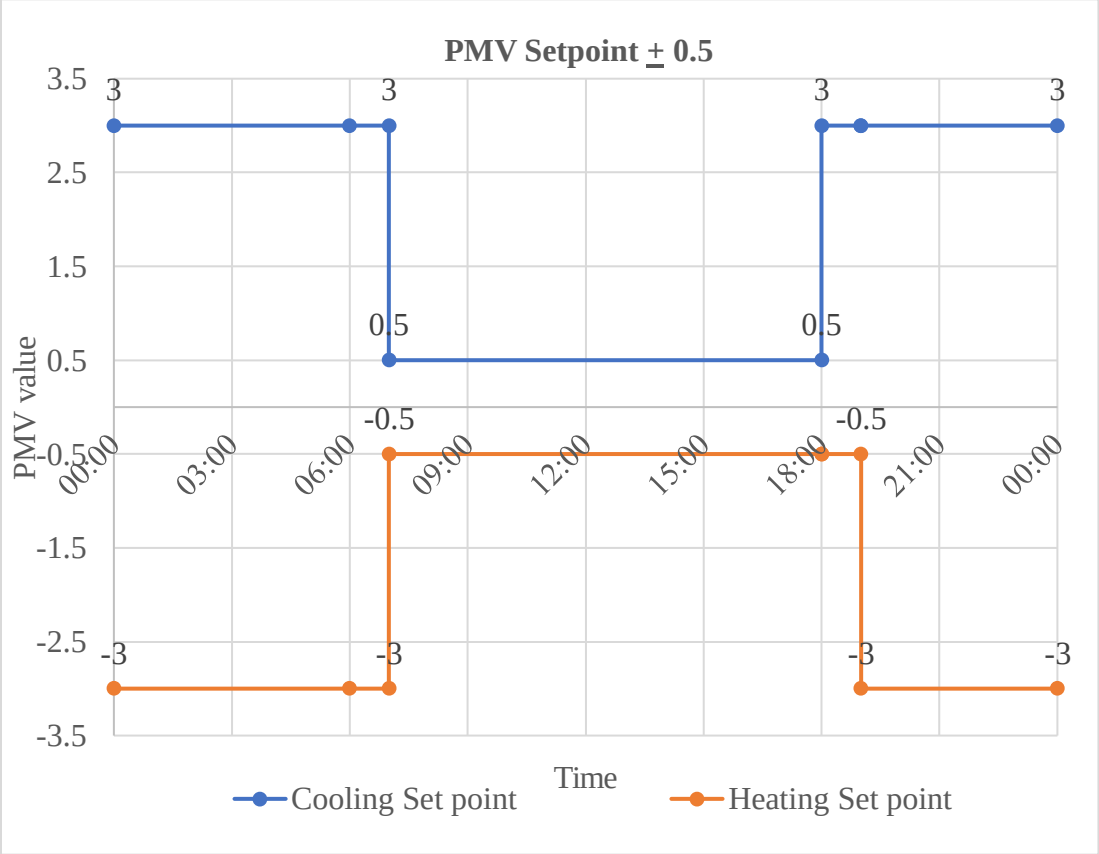

Figure 2.19: Cooling and heating setpoints of ± 0.5 PMV control in small building office

Figure 2.19 shows cooling and heating setpoints the PMV control assumes based on the thermal sensation scale. During business days, the heating PMV setpoint, represented by the orange line was maintained at -0.5 and cooling setpoints, represented by the blue line was maintained at +0.5. While at unoccupied times, the PMV value was allowed to float between ±3.

2.8.2: Case-2: PMV set-point of ±0.4

The second case of PMV setpoint ± 0.4 was used to study the sensitivity of the PMV control and its relation to comfortable hours and energy usage.

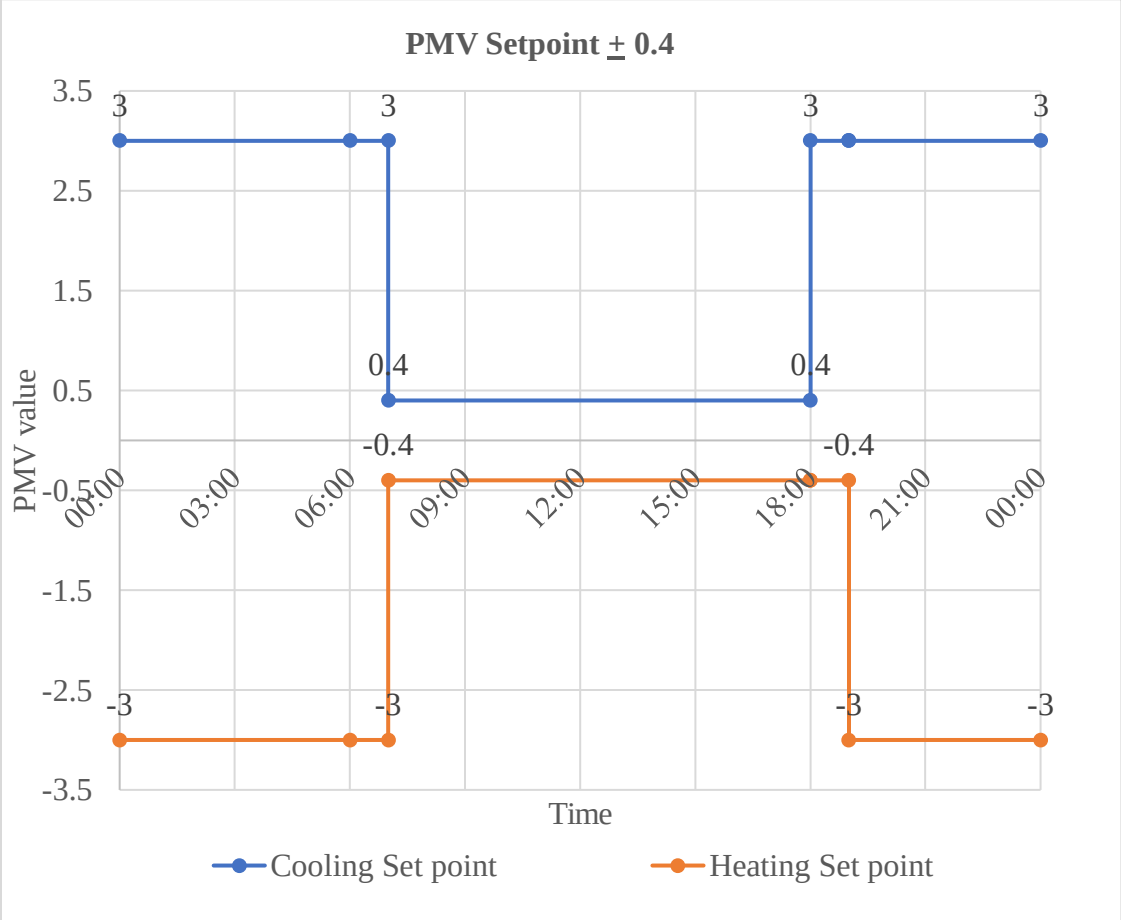

Figure 2.20: PMV setpoints of ±0.4 in small building office

Figure 2.20 shows PMV setpoints of ±0.4 at occupied conditions in small building office. During business days, the heating PMV setpoints, represented by the orange line in the figure was maintained at -0.4 and cooling setpoints, represented by the blue line at +0.4. While at unoccupied times, the PMV value was allowed to float between +/-3. The results of the simulations between conventional thermostat settings

and PMV based control settings in small building offices to 3 different locations are presented in the results section.

2.9 Estimating Occupancy from an IR camera

The primary goal of this present study was to determine a binary occupant signal from a captured IR image. As the detection of an occupant in an IR image poses several advantages for building management systems, our goal was to use open-source code to detect a person in an IR image.

Unlike traditional programming that requires specific codes to process the functions required by the user, machine learning focuses on data analysis rather than coding. Deep learning was a technique that evolved from machine learning, which imitates the functions of the human brain. The human brain's most unique characteristic is pattern recognition that can process and differentiate information. Deep learning algorithms use the same concept to carry out similar tasks in machines. Whenever new information is received, the brain compares it to known patterns and makes decisions. The deep learning algorithms employ the same concept using neural networks. A neural network is a type of model that can be trained to differentiate patterns. It consists of layers that include input, output, and at least one hidden layer. Figure 2.21 shows an example of a test image of a dog and the network predicting it to be a dog. The neurons of each layer learn progressively from the data. The neurons respond to edges, shapes, and objects to predict the output.

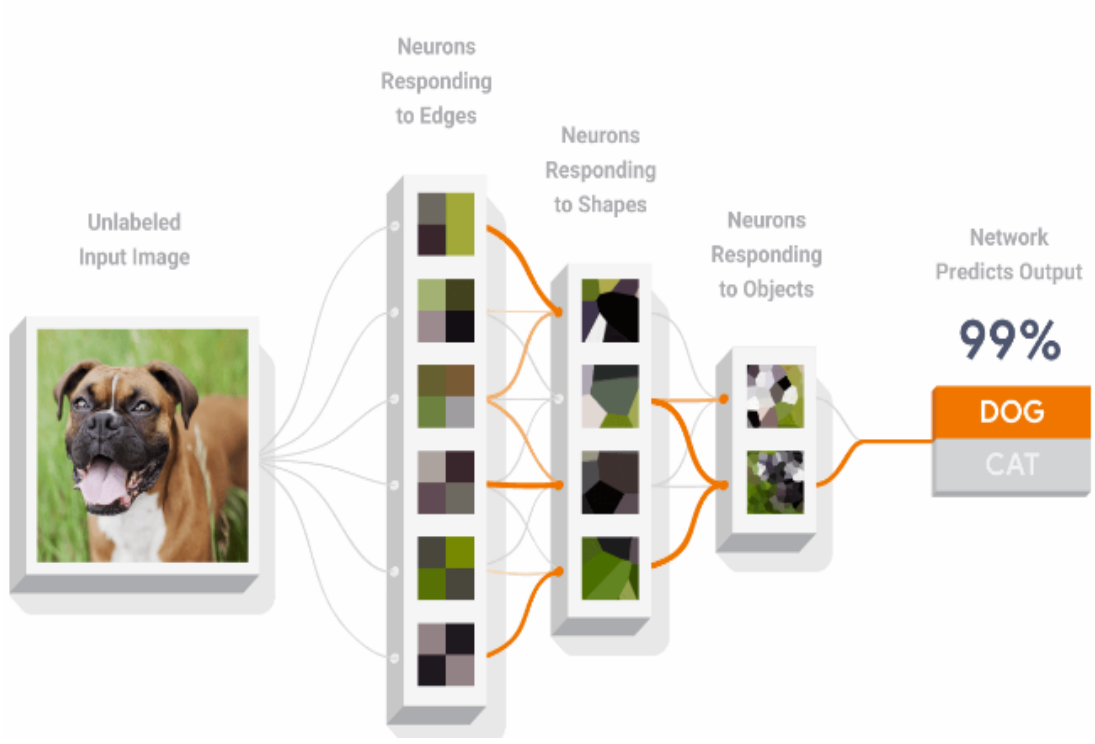

Figure 2.21: Anatomy of a neural network (Tensorflow, n.d.)

A commonly known platform is the TensorFlow object detection application program interface (API). TensorFlow is an open-source platform for machine learning. TensorFlow object detection API is a powerful tool that can be used by beginners with little background in machine learning to classify images. It uses pre-trained models to detect objects. The API has five different models. We used a lightweight SSD MobileNet network model for our project. Mean average precision (mAP) is a score of the accuracy of the model. The higher the mAP score of the model, the faster the speed of detection accuracy, but the speed of running the code is lower. The dataset it uses for training is COCO (common objects in context). It contains 300,000 images of the 90 most common objects found around us.

The TensorFlow project has many useful framework extensions; one such is Object detection API. The TensorFlow Object Detection API is an open-source framework built on top of TensorFlow. The object detection code API used in this study was developed by Huang (Huang, et al., 2017). The repository was downloaded from Github, a host to open source projects owned by Microsoft Corporation. The code can be implemented and modified according to the user's application needs. The repository is maintained by individual researchers on Github. There are numerous open-source codes available in Github to detect humans in red, green, and blue (RGB) images. The TensorFlow API uses bounding boxes to detect objects in images or video based on pre-trained models. TensorFlow object detection API is widely used and many researchers discuss its capabilities and simplicity in usage. We relied on the API documentation, blogs, and tutorial videos to learn to run the API to detect objects in space (Jonathan, et al., n.d.) (PythonProgramming.net, n.d.) (Sutton, 2017). One such blog discussed an approach for identifying a human shape in infrared images (Shah, 2019). The blog discusses how to detect objects using infrared images or videos with TensorFlow object detection API. We used Spyder 3.3.6 to run the API and the version of Python used was 3.6.8.

The infrared images from FLIR C2 were used to check the detection capabilities and accuracy of the object detection API. The FLIR C2 has capabilities to capture radiometric and visual images at the same time. The MSX feature in the IR camera can be used to enhance the clarity of the thermal image by blending visual details in real-time. The quality of the thermal images generated with FLIR MSX technology is far better than that of thermal images. Four test case scenarios were used to detect the

occupant using the TensorFlow Object Detection code. The infrared images are single-channel images. The pre-trained algorithms of the API are trained on 3-channel RGB images and not for single-channel input. The infrared camera outputs were single-channel images and would not work with the code. Therefore, in this study, the author converted the infrared images into 3-channel inputs. The code could also be used to detect common objects in space. As our aim was to detect a person in the infrared image, we focused the test images on a person. The object detection API detects objects using bounding boxes and shows the accuracy of objects identified using percentage. The test images used for person detection was with FLIR MSX feature IR image and thermal image. Four scenarios were used with a person in a different position to test the algorithm. The results of person detection in IR images with MSX feature and thermal image using TensorFlow Object Detection API are presented in the results section.

CHAPTER 3 **: RESULTS**

At first, the results of the validation and verification of the IR camera's surface temperature measurements are presented. Thereafter, the results of the MRT and PMV value obtained in Excel are presented and verified with the center of built environments MRT and thermal comfort tool. Finally, the results of occupancy detection using IR camera and EnergyPlus simulations of comparing standard thermostats with PMV thermostats are presented in this section.

3.1 Validation Test of the IR camera

Table 3.1 shows the average temperature deviations between IR images and thermocouple measurements. Based on the results, the north wall, west wall, south window frame, and west window underestimated the surface temperatures compared to the thermocouple readings. The floor, ceiling, and south window overestimated the surface temperatures compared to the thermocouple readings. The average of the seven deviations is -0.22°F, which indicates a bias error of -0.22°F over the surfaces that were tested.

Table 3.1: Average temperature deviations from thermocouple measurements

ROOM SURFACES	Average temperature deviation from thermocouple measurements (°F)
North Wall	-1.23
West Wall	-0.8
Floor	0.21
Ceiling	0.88
South Window	0.248
South Window Frame	-0.69
West Window	-0.19

In addition, the spread of the calibration results in Table 3.1 are within the accuracy specification of +2 ℃ (+3.6 °F) publicized in the FLIR CX series manual.

3.2 MRT Tool

An MRT tool in Excel was developed to calculate the MRT value in relation to the occupant in space. The spreadsheet included two-dimensional coordinate translations of the test room geometry for REHVA view factor calculations. The recorded IR data for the baseline scenario was conducted during a sunny day in a winter month.

Table 3.2: MRT tool calculator

MRT Calculator							
origin (0,0)	South east	meters	Feet	Room	Orientation	2.7177	Height
Occupant position	X from east wall	0.9144	3.0001464	3.7338	South/North Wall	0.6	Below C.G
	Y from south wall	1.041	3.415521	4.3688	East/West Wall	2.1177	Above C.G
Room Surfaces	View Factors Rehva	Initial weighting factor	Final weighting factor	Surface Temperatures (°F)	(T^4) (°F)	(V.FxT^4)	
East Wall	0.234494254	0.237452817	0.237452817	69.8675	23828725.5	5658197.999	
South Wall	0.076257564	0.077219689	0.077219689	69.17125	22892988.79	1767789.476	
South Window	0.127594433	0.129204264	0.129204264	70.9165	25292349.44	3267879.391	
West Wall	0.059112738	0.05985855	0.05985855	68.365	21844156.16	1307559.518	
West Window	0.021149563	0.021416402	0.021416402	67.7665	21089205.72	451654.9121	
North Wall	0.058720072	0.05946093	0.05946093	69.755	23675620.62	1407774.422	
Floor	0.301928463	0.305737829	0.305737829	62.43942857	15199723.21	4647130.373	
Ceiling	0.108126131	0.109490335	0.109649519	68.641	22199050.94	2434115.25	
Total	0.987383217	0.999840817	1			20942101.34	
MRT	(V.FxT^4)^4	Temperature in fahrenheit	Temperature in celsius				
	67.64801603	67.64801603	19.80445335				

Table 3.2 shows the MRT tool calculator developed in Excel. A check for validating the view factor calculations is that the sum of all the view factors should equal one. Using REHVA equations the summation of view factors for all the surrounding surfaces was not one because of algebraic approximation of integration. The MRT value will not be accurate if the sum of the view factor fractions is not equal to one. The difference to unity of the computed view factors is corrected as an initial and final weighting factor so that the sum of all the computed view factors becomes one. Then, the final weighting factors are multiplied with the respective surface temperatures to the fourth power to calculate the final value for MRT using the MRT equation. The MRT result for the baseline scenario calculation was 67.6°F (19.8°C). The surface temperatures

of the room were in the range from 62.2°F to 70.9°F. The floor was at the lowest measured surface temperature in the room. The resulting MRT value is influenced primarily by the floor, east wall, and south window.

According to most building standards, window assemblies are more conductive than walls. The IDL test chamber window assemblies were in the range of R-2 to R-3 based on ASHRAE 90.1, 2007 standard. In this study, the measured room air temperature and calculated MRT had a difference of 0.2°C. They were both found to be almost equal in the baseline scenario. In the baseline scenario, the heat pump was only turned on a few minutes before the occupant test was performed and almost all the surrounding surface temperatures were in thermal equilibrium. This scenario would be similar to HVAC systems initializing after a setback condition. In such a situation, the surrounding surfaces would have similar temperatures. But in most office scenarios, the heating, and cooling load profiles during the office working hours can vary due to occupants, solar radiation through windows, and even due to appliances. A person seated near to a window would feel uncomfortable as to a person seated near the center of the room due to differences in MRT. The focus of this study was to develop a method to measure MRT using infrared cameras and did not focus on the accuracy of the experimental setup of the test chamber.

3.2.1 Verification of the MRT value

ASHRAE standard 55-2017 updates mention web-based software to calculate MRT and solar radiation effects on occupants in buildings (Arens, Heinzerling, & Paliaga, 2018). The center for the built environment (CBE, University of California, Berkeley) has developed a graphical tool for modeling the spatial resolution for mean radiant temperature within space. We used this tool to verify our MRT estimate with the

baseline scenario. The surface temperatures were entered, and the test chamber was modeled in CBE, MRT tool. The occupant position was selected as seated, the emissivity of surrounding surfaces was kept at 0.95. As our Excel tool calculator did not consider solar radiation factors, the solarcal in the CBE MRT tool was set to 0.

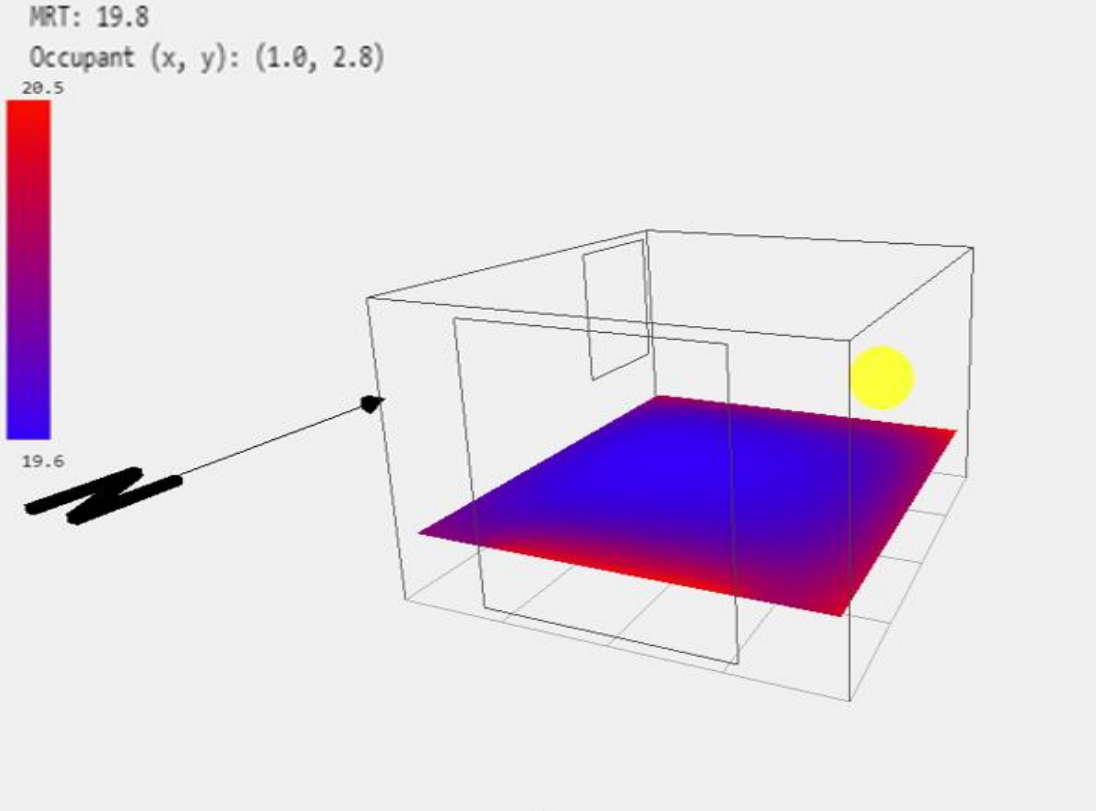

Figure 3.1: IDL test chamber modeled in CBE MRT tool

Figure 3.1 shows the CBE MRT tool we used to calculate the MRT result for the baseline test scenario. The geometry and surface temperatures of the test room were modeled in the CBE MRT tool. The cursor in the geometry related to the occupant position and was adjusted to the occupant's position in the baseline scenario. The MRT scale in the room was in the range of 20.5°C to 19.6°C. From studies, the effect of MRT

is more prevalent at high outdoor temperatures and rooms with windows facing southeast and southwest. These windows showed above-average temperatures and the surrounding wall temperatures were not uniform. The size of the windows and the duration of solar radiation entering the room affect the difference between air temperature and MRT (Walikewitz, Jänicke, Langner, Meier, & Endlicher, 2015). The red region in the model denoted the higher temperature and the blue region in the tool denotes colder regions. The MRT effect in the test chamber is higher in the southeast and southwest regions of the room denoted by the red regions modeled in the CBE MRT tool. The CBE MRT tool inputs are in S.I units. The MRT result calculated by the CBE MRT was 19.8°C. This value agreed with the MRT value calculated by the Excel spreadsheet (19.8°C).

3.3 PMV-PPD Results

The PMV Excel tool was developed in Excel as mentioned in the methods sections and was linked with the MRT spreadsheet. The calculated PMV-PPD value for the baseline scenario was -0.794 and PPD of 18.2%. The results indicated that the occupant was uncomfortable and felt slightly cold. A PMV value of -0.794 indicated the space needed to be heated to bring the PMV value within a comfortable range of -0.5 to +0.5. A PPD value of 18.2 indicated, 18.2% of the people in the space were uncomfortable. As per ASHRAE standards, a PPD value of 10% is considered acceptable. The PMV-PPD value obtained for the baseline scenario was not in the comfort range.

3.3.1 Verification of the PMV-PPD value

The Lawrence National Berkeley lab has developed an online thermal comfort tool with an option to choose the comfort method to predict if the comfort parameters were within ASHRAE Standard 55-2017. We validated our PMV- PPD results developed in Excel with CBE Thermal Comfort Tool.

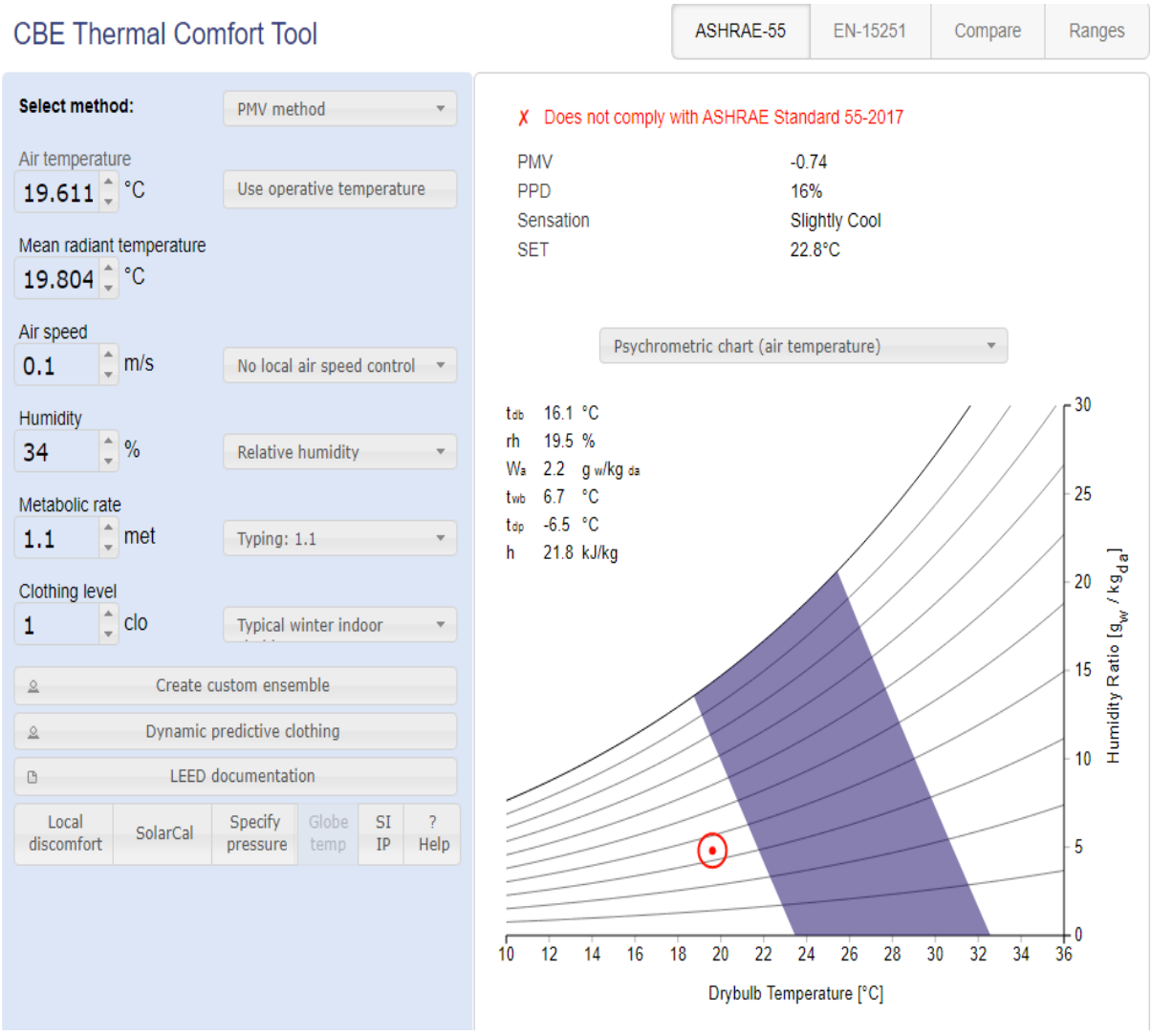

Figure 3.2: CBE Thermal Comfort Tool

Figure 3.2 shows the CBE Thermal Comfort Tool we used to validate our PMV Excel calculator. The purple shaded area on the psychometric chart represents a comfort

band, while the red dot indicated current conditions. The thermal comfort parameters measured and assumed for the baseline scenario was used in the CBE thermal comfort tool. The results indicated that the PMV value did not comply with the ASHRAE Standard 55-2017. The thermal comfort tool indicated a PMV value of -0.74 and PPD of 16%. The CBE thermal comfort tool results indicated the occupant felt slightly cool and the air temperature required to correct the disparity was 22.8°C.

Table 3.3: PMV-PPD value comparisons

	PMV Excel Tool	CBE Thermal Comfort Tool
PMV	-0.794	-0.74
PPD	18.20%	16%

Table 3.3 shows the comparisons of PMV-PPD value we obtained from the developed excel tool with the CBE thermal comfort tool. The PMV value from the Excel tool shows slight differences but was in general agreement with the value calculated in the CBE Thermal comfort tool.

The PMV results will call for heating and cooling modes to make the space within comfortable levels. The PMV value is used as a logic to take corrective measures or to determine if space is in the comfort range. The obtained PMV value of -0.794 was rounded off to -1. The PMV value of -1 will call the system to heat the space until the scale reaches -0.5. The BASstat thermostat was accessed via computer using wireless communication and using the BACnet discovery tool the BACnet device was discovered. The BASstat thermostat included 120 objects. Some of the objects which were of interest to our project goals were occupied and unoccupied setpoint in cooling and heating mode,

fan control, heating and cooling set points and occupancy. The setpoints of the thermostat were changed using object write value property to the call for heating mode.

3.4 Occupancy Detection Using IR Cameras

The results below discuss person detection using an IR camera (FLIR C2) at different positions. Infrared images in grayscale were used as inputs to the object detection algorithm. FLIR C2 has an infrared and digital camera. Figures below are IR images showing person detection in an IR image with MSX feature and an IR image without the MSX feature.

Figure 3.3: Standing person detected using a deep learning technique

Figure 3.3 shows a standing person detected in an infrared image captured by FLIR C2. The image on the left shows a thermal image with an MSX feature and a person detected with 98% certainty. The image on the right shows a thermal image with a person in a standing position and detected with 85% certainty.

Figure 3.4: Seated person detected using a deep learning technique

Figure 3.4 shows a seated person detected in an infrared image captured by FLIR C2. The image on the left shows a thermal image with an MSX feature and a person detected with 62% certainty. The image on the right shows a thermal image with a person in a seated position. The person in the thermal image was not detected by the object detection algorithm.

Figure 3.5: A seated person with a close-up portrait on a face detected using a deep learning technique

Figure 3.5 shows a seated person with a close-up portrait on a face detected using deep learning techniques in an infrared image captured by FLIR C2. The image on the left shows a thermal image with an MSX feature and a person detected with 66% certainty. The image on the right shows a pure thermal image and detected with 69% certainty.

Figure 3.6: Standing person captured by an IR camera from a far distance

Figure 3.6 shows a standing person captured by FLIR C2 at approximately 5 meters from the camera. The image on the left is captured with the MSX feature and the image on the right is without the MSX feature. The object detection algorithm did not detect a person in either of the IR images.

All four scenarios were used to understand the object detection algorithms prediction capabilities. In Figure 3.6, the algorithm failed to detect the person in the image as the person was captured at a distance. This could be due to the lack of clarity of the captured image, or due to the lack of training data under similar conditions. In Figure 3.5, the seated person with a close portrait on the face, both the input images detected with almost the same confidence. In Figure 3.4, the seated person that was captured sideways, the IR image with the MSX feature detected the person and the thermal image could not detect the person in the image. In seated positions, a fraction of the body was

not captured in the image and hence the code detects the person with less certainty. In Figure 3.3, the IR image with the person standing and closer to the IR camera detected with the highest certainty among all the scenarios. The IR image with the MSX feature detected with higher certainty. As the person was closer to the IR camera and the whole-body being captured in the frame, the algorithm was able to detect the person with better certainty compared to other scenarios.

Hence, it was understood that using an open-source object detection API on infrared images, a person could be detected as with an RGB image. From the test images, the IR images with the MSX feature showed better results. The algorithm could also detect the person and common objects while connected to a live stream video from the FLIR C2 camera.

3.5 EnergyPlus Simulation Results

The EnergyPlus simulation for small prototype buildings was simulated for the whole year and results were analyzed for occupied office conditions. Two different PMV setpoints were compared to standard thermostat setpoint. Case 1 was analyzed with a PMV setpoint of ± 0.5 and case 2 with a PMV setpoint of ± 0.4 to compare the energy usage and comfort hours with PMV control type to the conventional thermostat.

3.5.1 Case 1: PMV setpoint ±0.5

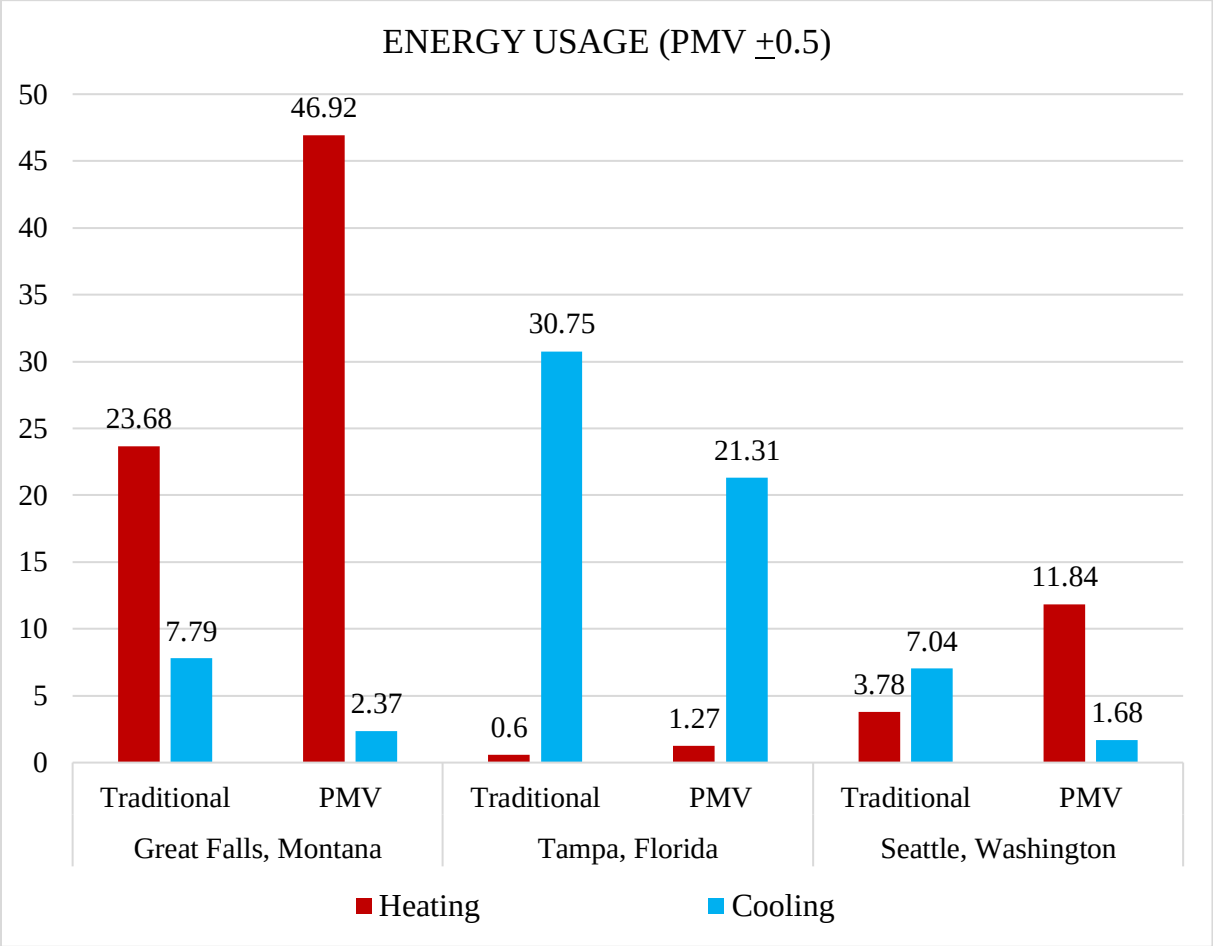

Figure 3.7: Heating and cooling energy comparisons with conventional thermostat setpoints and PMV setpoint of ± 0.5

Figure 3.7 shows the heating and cooling energy comparisons between the conventional (Traditional) thermostat and PMV control setpoint of ±0.5 in 3 locations in the United States. Across all the locations the energy consumed for heating was higher and energy consumed for cooling was lower with PMV control. In Great Falls, Montana there was a total of 57% increase in energy with PMV control. In Tampa, Florida there was a decrease of 28% energy with PMV control and in Seattle, Washington the total energy increased by 25% with PMV control type.

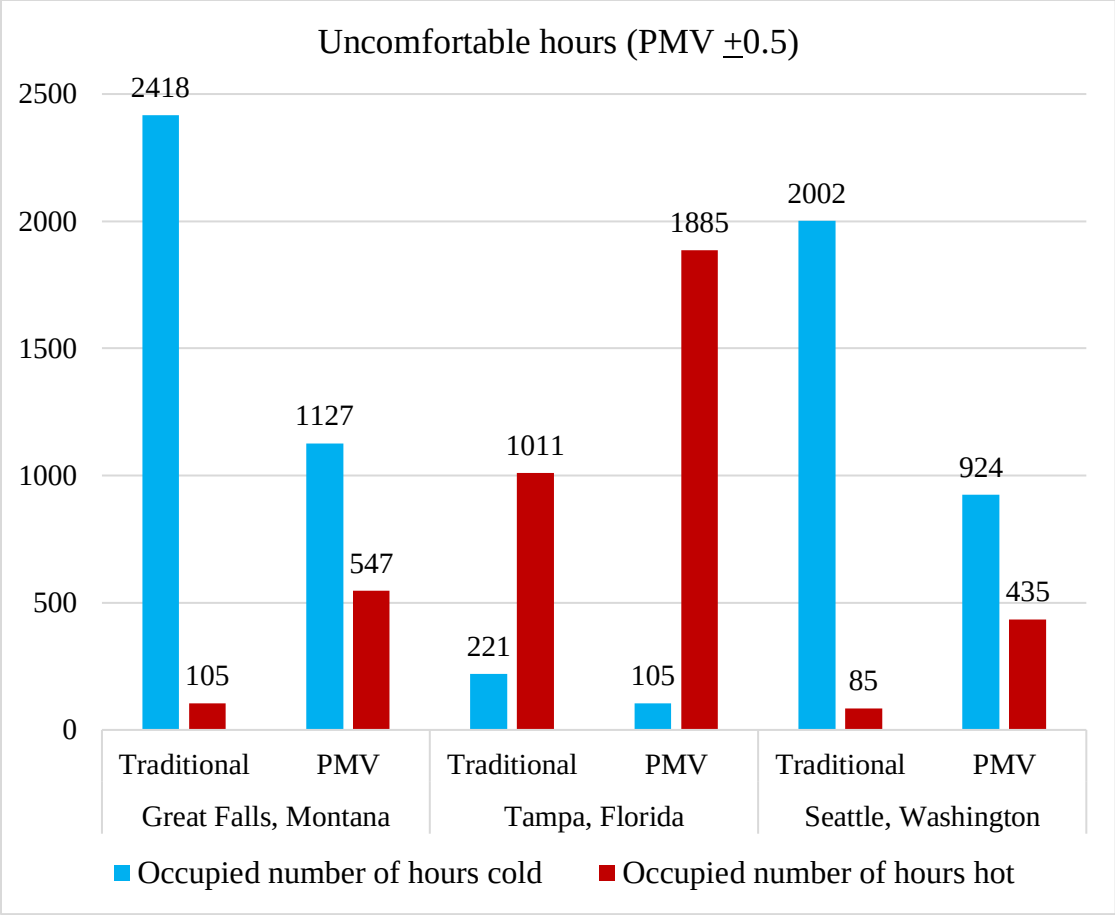

Figure 3.8: Number of uncomfortable hours with PMV set-point, ±0.5

Figure 3.8 shows the results of the number of occupied uncomfortable hours between simulated conventional (Traditional) thermostatic control setpoints and PMV control settings of ±0.5 for 3 locations in the United States. The heating energy indicated with a red bar in Figure 3.7 correlates with the occupied number of hours cold indicated in the blue bar in Figure 3.8. The cooling energy indicated with a blue bar in Figure 3.7 correlates with the occupied number of hours hot indicated by the red bar in Figure 3.8. Across all the locations, the total number of people that felt cold with standard control settings was higher than PMV control settings and the total number of people that felt hot was higher with PMV control type. In Great Falls, Montana the total number of

uncomfortable hours decreased by 34%. In Tampa, Florida the total number of uncomfortable hours increased by 62%, and in Seattle Washington, the total number of uncomfortable hours decreased by 35%. In all the locations, people that felt colder in space were lower with PMV control, and people that felt hot with space were higher with PMV thermostat. To further understand the characteristics of the PMV control set-point a second case was analyzed.

3.5.2 Case 2: PMV setpoint ±0.4

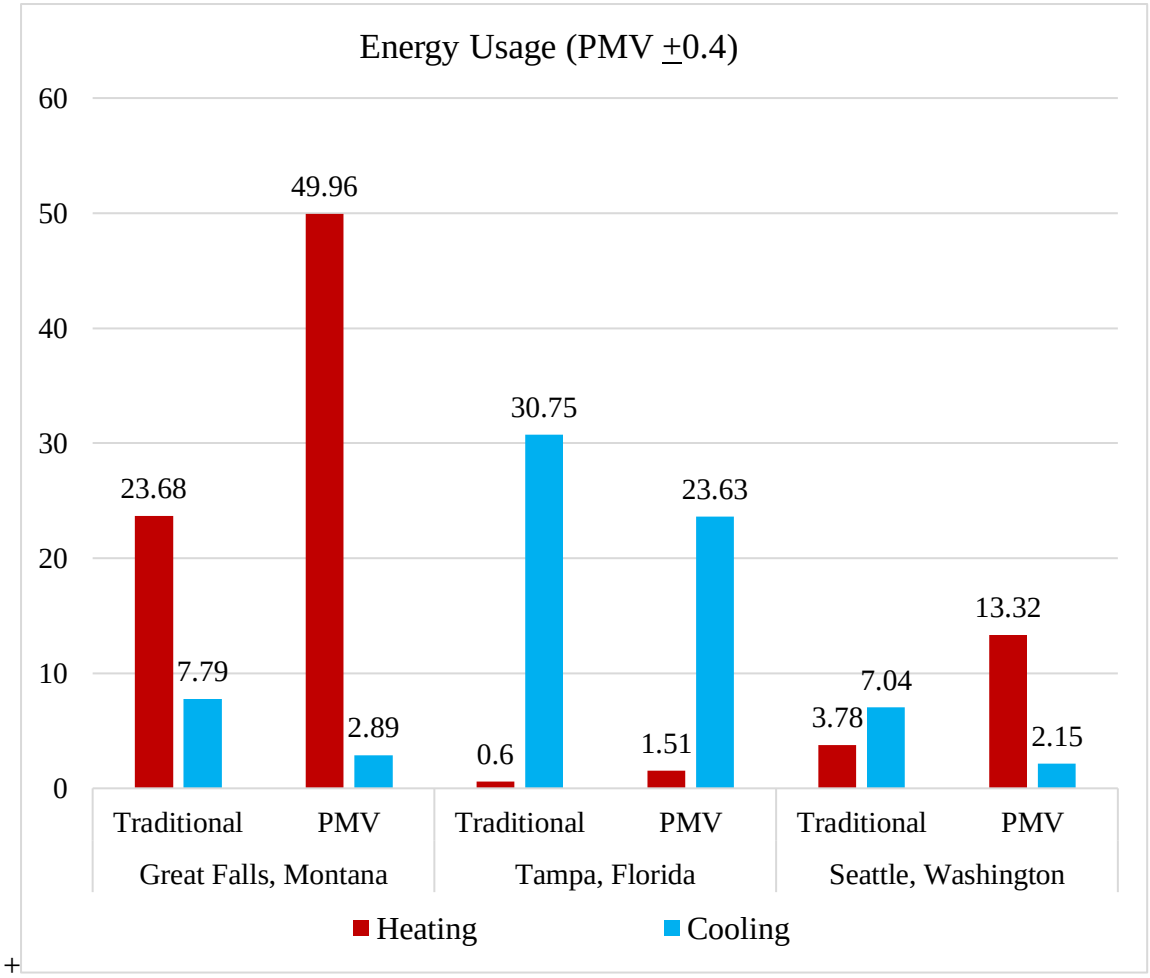

Figure 3.9: Heating and cooling energy comparisons between conventional thermostat setpoints and PMV setpoint of ±0.4

Figure 3.9 shows the heating and cooling energy comparisons between the conventional (Traditional) thermostat and PMV control setpoint of ±0.4 for 3 locations in the United States. Across all the simulated locations the energy consumed for heating using PMV control was higher and energy consumed for cooling was lower for PMV control. With PMV ±0.4 setpoints, Great Falls, Montana there was a total of 68% increase in energy with PMV control. In Tampa, Florida there was a decrease of 20% energy with PMV control and in Seattle, Washington the total energy increased by 43% with PMV control type.

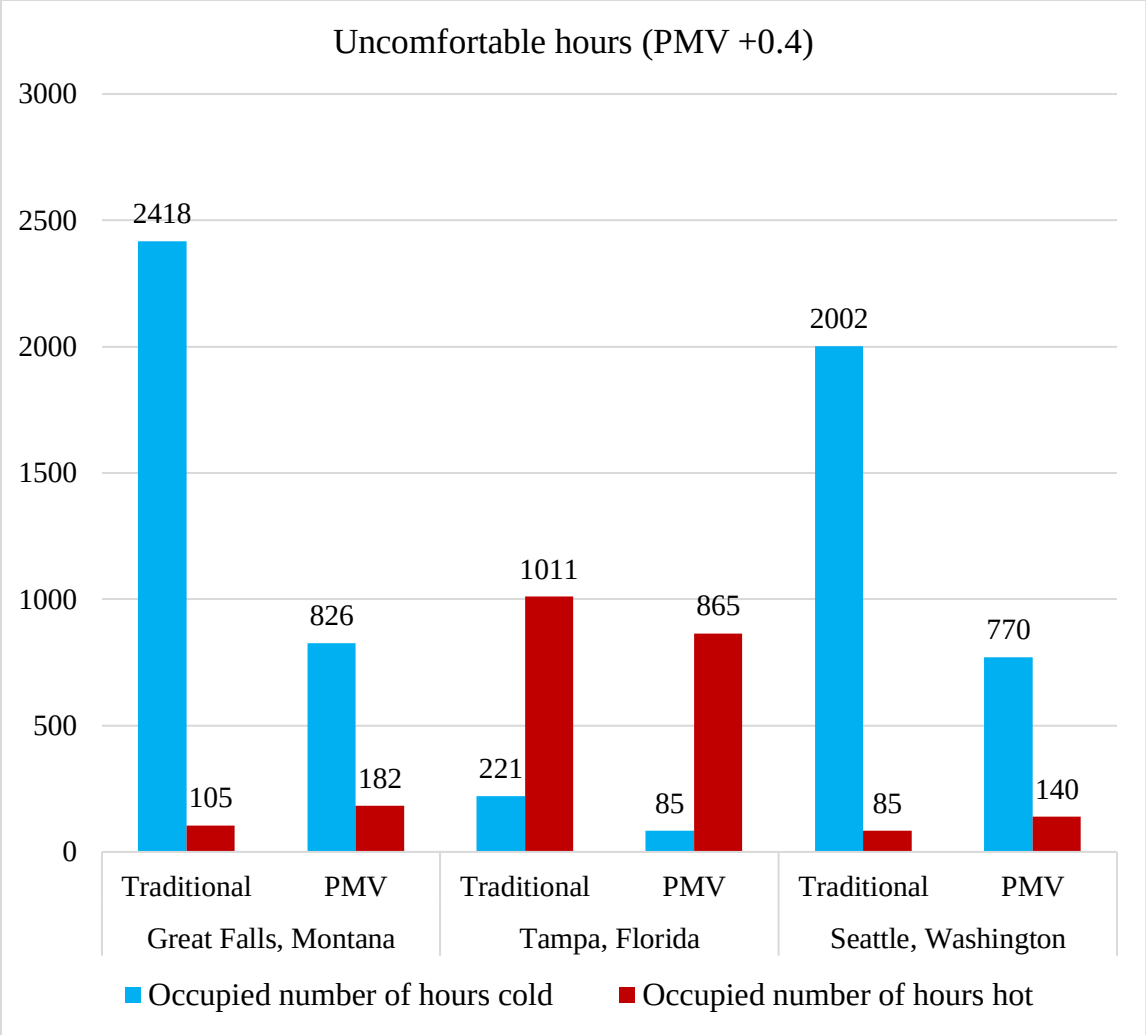

Figure 3.10: Number of uncomfortable hours with PMV set-point, ±0.4

Figure 3.10 shows the results of the number of uncomfortable hours between simulated conventional (Traditional) thermostatic control setpoints and PMV control settings of ±0.4 for 3 locations in the United States. Across all the locations, more people that felt colder with conventional control settings than with PMV control settings. The total number of people that felt hot was slightly higher in Great Falls and Seattle and was lower in the Tampa region using PMV controls. In Great Falls, Montana, the total number of occupied uncomfortable hours decreased by 60%. In Tampa, Florida the total

number of occupied uncomfortable hours decreased by 23% and in Seattle, Washington the total number of occupied uncomfortable hours decreased by 56%. With ±0.4 PMV set-points, uncomfortable hours reduced considerably for the total number of people that felt hot in occupied conditions. Hence, varying the PMV setpoints improved the comfort conditions of occupants in space with a 7.2% increase in energy usage at Great Falls, Montana, 11.3% increase in energy usage in Tampa, Florida, and 14.4% increased energy usage in Seattle, Washington with the conventional thermostat. Hence, narrowing the PMV setpoints decreased the uncomfortable hours significantly but increased energy use.

In both cases, the cooling energy used was lower than the heating energy and the energy usage correlated to more people feeling hot and fewer number of people feeling cold as compared to the conventional thermostat. The small building prototype model has a 44% window to wall ratio. With the inclusion of MRT as one of the governing parameters in the PMV control type, the HVAC systems account for the heat loss of all the windows and tends to keep the spaces warmer.

CHAPTER 4 **: DISCUSSION AND CONCLUSION**

4.1 Importance for Comfort Control Strategy in Buildings

Since the 21st century, building electro-mechanical systems have been developed for maintaining a comfortable environment for occupants indoors. The built environment is the largest growing sector and consumes the most energy (40%) overtaking the transportation and industrial sectors. At present, several researchers widely recognize occupant behavior as a major contributing factor to uncertainty in building performance (Virote & Silva, 2012) (Yan, et al., 2015) (Buso, Fabi, Andersen, & P.Corgnati, 2015) (Zhou, Qiao, Jiang, Sun, & Chen, 2016) (Rinaldi, Schweiker, & Lannone, 2018). Building standards and practices in the past often did not address the thermal comfort needs of humans in the sustainability context of the built environment (Horr, et al., 2016). This led to the designing of building systems primarily focused on energy efficiency in operation and led to a higher number of user comfort issues in buildings. Karmann conducted a study from 52,980 occupants in 351 office buildings mainly in North America over the period of 10 years and results indicated that 43% percent of the people are thermally dissatisfied and HVAC systems or controls fail to provide adequate conditioning for occupants (Karmann, Schiavon, & Arens, 2018).

The building control research community often focuses on reduced energy demand through optimal operation, while the thermal comfort research community primarily focuses on achieving occupant satisfaction (Tommaso, 2019). There needs to be a balance between both the fields in order to achieve a sustainable built environment. Both the fields are interdependent, and an energy-efficient building operation cannot be achieved without accounting for human comfort. The main energy driver in buildings is

human comfort. Hence, building controls that are primarily human comfort centric can reduce thermal comfort complaints in buildings and can also save energy. Various studies have shown consistent relations between thermal comfort and energy efficiency (Kwong, Adam, & Sahari, 2014), (Kang, et al., 2010) (K.E, T.Mathew, & Jacob, 2018) (Gao, Li, & Wen, 2019). A man's thermoregulatory system is more complex and comprises of intricate control principles than actual control systems in practice (Hensel, 1981). The standard practice of measuring air temperature alone misses out on several parameters that determine human thermal comfort indoors.

It is necessary for HVAC controls to address and integrate with human psychological and physiological needs. Even though thermal comfort literature has existed in the standards, the implementation of a comfort-based control in buildings has been scarce. Much of the researchers have limited their studies due to a lack of low-cost tools and integration methods to obtain indoor environmental data. The recent dramatic reduction in the cost of infrared cameras means they can feasibly be used as a part of a building's control system. The ability to predict human radiative heat exchange in a heterogeneous indoor environment could improve the productivity and thermal comfort of occupants and in turn save energy (Kubaha, Fiala, & Lomas, 2003). The capability of an IR camera in measuring radiative heat exchange indoors and its capability of integration with a comfort control strategy makes it ideal for its incorporation in smarter building controls.

4.2 Proof-of-Concept

This study demonstrated that it is possible to use an inexpensive IR camera to predict comfort and occupancy in an office and run a thermostat based on those comfort predictions. Datcu conducted an experimental study on the surface temperature measurements by infrared (Datcu, Ibos, Candau, & Matteï, 2005). As opposed to the standard method of measuring surface temperature using a thermocouple, the IR camera is a non-intrusive technology and does not impact the temperature profile of the object being measured. It does not produce any harm to the user or to the surroundings. In this study, the IR camera was able to precisely acquire surface temperatures within the range of $\pm$1.23°F to that of thermocouple readings. The measurement parameters in the IR camera; emissivity and reflectivity were adjusted to determine accurate radiometric values indoors. The distance measurement parameter did not influence the radiometric value from the IR camera and was set to zero in this study. These acquired surface temperature values from an IR camera were imported into an Excel MRT tool for PMV calculation. The Excel MRT and PMV tool calculations were in excellent agreement with the results from CBE thermal comfort tools. This proved that our methodology of a PMV based comfort control is feasible for controlling indoor temperatures.

Our study proved that it is possible to recognize an occupant in low-resolution IR images using the TensorFlow Object Detection API developed by Google's artificial intelligence team with a minor change in code. Cosma study suggested that IR cameras that have capabilities to combine visual and thermal modes can be used to drive HVAC systems in terms of detecting occupants and modeling thermal comfort (Cosma & Simha, 2018). IR cameras can sense radiation emitted by an object in the infrared spectrum

which cannot be achieved with a visual camera and information such as color, geometry, and texture is not available in an IR camera (Jiang, et al., 2004). Several researchers have proved the fusion of IR and visual images for detection has superior detection results (Han & Bhanu, 2003) (Jiang, et al., 2004). From the test images in this study, results showed that IR images with thermal and visual modes combined detected occupant in space with better certainty. A large portion of energy usage that is wasted in buildings comes from unoccupied rooms (Meyers, D.Williams, & Matthews, 2010) (Martani, Lee, Robinson, Britter, & Ratti, 2012). Sun conducted an energy simulation study and results showed an overall site energy savings up to 41% by integrating occupant behavior measurements (Sun & Hong, 2017). In this study, the IR camera outputs were integrated into a thermostat signal. The inclusion of an IR camera with a thermostatic control can serve as an added intelligent sensor that can detect occupants, acquire radiometric data, and model thermal comfort to drive HVAC systems efficiently.

4.3 PMV Control Simulation

The Department of Energy software, EnergyPlus simulations were used to run comparison studies on energy usage and the number of hours uncomfortable in a PMV based thermostat and a conventional thermostat in a small office prototype. Two simulation cases of PMV setpoints were used to analyze the characteristics of comfort control. The first PMV setpoints analyzed were $\pm$0.5, which is the standard comfort scale as per ASHRAE standards in which maximum occupants in space are satisfied (>80%). The second PMV setpoints analyzed were $\pm$0.4 to further reduce the uncomfortable hours obtained in $\pm$0.5 PMV setpoint simulation. In both cases, the cooling energy consumed

by the PMV based control was lower than the conventional thermostat and the heating energy used to keep the space comfortable was higher in a PMV thermostat.

At present, over-cooling issues in commercial buildings in the United States is common. It wastes energy and results in occupant discomfort (Zhang, et al., 2018). Bennett conducted field studies of 37 small and medium commercial buildings throughout California and results showed that offices were regularly overcooled in the summer (Bennett, et al., 2012). From our EnergyPlus simulation results, the total number of occupied hours that people felt colder with the PMV control was lower than the standard thermostat. The conventional thermostat kept the office spaces colder throughout the year. This has serious implications on the energy cost profile in buildings. Derrible using data from US Energy Information Administration (EIA) in a simulation study calculated an energy cost of 13,929 GWh, an environmental cost of 57, 125 kt CO2e and financial implication of 10 billion dollars, in total estimated a loss of 8% (Derrible & Reeder, 2015). From our simulation results, the PMV based control kept the spaces more thermally comfortable. The control trends to keep the space warmer and significantly lowered the overcooling issues as compared to the conventional thermostat findings. The comfort-controlled strategy implemented in buildings can address overcooling issues and save energy.

Kang performed a simulation study comparing PMV-based comfort control and conventional thermostatic control under similar conditions and results showed that the energy-saving potential increased with lower mean radiant temperature and reduced with higher mean radiant temperature conditions and results suggested that the PMV control is still a practical strategy to achieve both thermal comfort and energy savings (Kang, et al.,

2010). With the incorporation of MRT as one of the governing parameters in the control strategy, the thermostat is more sensitive to the surrounding temperatures, responding to cold surface temperatures of windows in the winter. The MRT parameter in the control would allow for wider air temperature setpoints in the summer, thus saving cooling energy.

Thermal comfort complaints are the highest occurring complaints in commercial buildings in the United States. With proper implementation of better-performing controls for HVAC systems, there is a potential to reduce labor costs of HVAC maintenance by 20% (Federspiel, 1998). The conventional thermostat trends to achieve uniform set-point temperature throughout the conditioned space. Madsen found variation in indoor temperatures between 0.5°C and 3.9°C for a 24 hours period at constant set-points (Madsen, 1987). The conventional thermostat consistently keeps conditioning the space leading to comfort problems in the space and increasing energy usage. In addition, a thermostat placed away from a room receiving solar gain will be warmer than the rest of the space and will make a poor judgment of the thermal comfort needs of the occupants. A control that is not occupant centered in operation leads to indirect waste of the energy used in buildings. The PMV control logic incorporates six parameters that govern thermal comfort in humans and addresses the comfort needs of the largest number of people in the space. In our simulation study, it was found that in both cases the energy used for heating was higher and the energy used for cooling was lower. The PMV control tends to keep the space warmer than the conventional thermostat. The PMV control addressed the overcooling issues that are dominant in conventional thermostats in all the locations and in Tampa, Florida there was a 28% reduction of energy use. The implementation of a

PMV control for space conditioning is human comfort centered in operation and can simultaneously reduce energy cost and its implications to our environment. A comfort-based control is superior in performance to conventional air-based control in buildings.

Our study proves that our proposed strategy is feasible and can be implemented in buildings with automation techniques. The idea of implementing this control scheme in building control is to supply what is essential and, to minimize waste.

CHAPTER 5 : **FUTURE WORK**

A conscious design and adaptation that has evolved from past problems and addresses the present and future needs are essential. It is crucial for buildings to be human-centric and efficient in design and operation. The application of an infrared camera integrated into the building control system poses several advantages. An IR camera can be programmed to detect an occupant in space, perform security surveillance even during night conditions, locate a person in the room, detect hot and cold spots in space, and model human thermal comfort. With an IR camera's capability to identify people in the room, could also extend its application to targeted cooling and heating in a space. The conventional method to detect occupancy and regulate ventilation systems is to use a CO_2 sensor. An IR camera can serve both these functions and determine the MRT in a space. Infrared cameras at present are used by researchers and engineers to detect moisture problems and internal building defects (E.Barreira, R.M.S.F.Almeida, & Delgado, 2016) (Fox, Goodhew, & Wilde, 2016). Many of these IR camera applications could be combined into a single product and incorporated into building controls to manage the built environment intelligently. This would reduce the number of sensors needed in a space and could reduce installation costs. However, much research is needed into integrating all these aspects of an IR camera into a building management system.

The future of smart buildings will require building management systems to have efficient and decisive controls that are human-centric in operation and intelligent in sensing ambient conditions. This study focused on determining the MRT parameter accurately in the PMV model. The accurate measurement strategies and feasibility of the remaining five thermal comfort parameters indoors can bring the comfort-based

thermostat closer to commercialization. The measurement parameters settings of an IR camera need to be automated, which would require real-time ambient temperature input and angular measurements for surfaces in the room that are highly reflective. The placement of the IR camera in the room for surface temperature measurement requires further research. In our study, the room geometry was modeled in Excel and the MRT values were calculated manually for each occupant position. Guo used an IR sensor coupled with a range finder to output a three-dimensional map of the room's surface geometry (Guo, Teitelbaum, Read, & Meggers, 2017). An IR control system that could automatically map a room and calculate MRT with respect to the conditioning requirements can be adaptable at large for a wide range of commercial buildings. The two personal factors in the PMV model (clothing level and metabolic activity) were assumed in our model based on typical office conditions. These parameters were captured in real-time by Zang using machine learning algorithms and had a great effect on the personal thermal comfort model (Zang, Xing, & Tan, 2019). Researchers have used IoT sensors to collect, store, and process the ambient data for the calculation of thermal comfort indoors (Park & Rhee, 2018) (Zang, Xing, & Tan, 2019) (Zhao, Genovese, & Li, 2020). At present, with the growing trends in IoT sensors, the implementation of a thermal control strategy is feasible in buildings at a lower cost.

Emerging technologies are highly influenced by open-source software. Users are free to learn, test, improvise, and develop applications and products. This is ideal for researchers to overcome the limitation of expensive tools and enables new assessment methods for smarter building controls. Technological solutions that can be made cheaper can be implemented in a wider population. The future of smart buildings will be largely

IoT-based. It enables the integration of real-world data into the digital world. At present, IR cameras that are smaller than a dime and one-tenth of the cost of a traditional IR camera are available. Such an IR camera that can be coupled along with open source tools and IoT sensors will be accurate in determining thermal comfort conditions indoors with several additional advantages such as control of lighting systems and active facades in a space. The Internet of Things (IoT) combined with Artificial Intelligence capabilities can bridge the gap between thermal comfort control and optimal energy usage in buildings. The goal of using IR cameras in building controls is to bring the concept of infrared-enhanced thermostats closer to commercialization. Combining the findings and implementation techniques different researchers used for comfort-based building control, the system can sense the surroundings with better intelligence and act in response to human thermal needs and reduce the impact of energy used in buildings. Once automated, this PMV logic using IR cameras can be scaled to multiple rooms or individual buildings. However, the integration of all these system processes and communication into an efficient building management system still requires much research.

REFERENCES

169-2013, A. S. (2013). *Climatic Data for Building Design Standards. American Society of Heating, Refrigerating, and Air-Conditioning Engineers.* Atlanta, Georgia: ASHRAE 2013.

A.Fokaides, P., AndriusJurelionis, LauraGagyte, & A.Kalogirou, S. (2016). Mock target IR thermography for indoor air temperature measurement. *Applied Energy*, 676-685.

Aghniaey, S., & M.Lawrence, T. (2018). The impact of increased cooling setpoint temperature during demand response events on occupant thermal comfort in commercial buildings: A review. *Energy and Buildings*, 19-27.

Akula, A., Shah, A. K., & Ghosh, R. (2018). Deep learning approach for human action recgnition in infared images. *Cognitive Systems Research*, 146-154.

Alfano, F. R., Isola, M. D., Palella, B. I., Riccio, G., & Russi, A. (2013). On the measurement of the mean radiant temperature and its influence on the indoor thermal environment assessment. *Building and Environment*, 79-88.

ANSI/ASHRAE. (2013). Thermal Environmental Conditions for Human Occupancy. *Standard 55-2013*.

ANSI/ASHRAE/IES Standard 90.1. (2016). *Energy Standard for Buildings Except Low-Rise Residential Buildings.* 2016 ASHRAE.

Arditi, D., & Nawakorawit, M. (1999). Issues in Building Maintenance: Property Manager's Perspective. *Journal of Architectural Engineering*, 117-132.

Arens, E., Heinzerling, D., & Paliaga, G. (2018). *Sunlight and Indoor Thermal Comfort.* ASHRAE JOURNAL.

ASHRAE. (2013). *ASHRAE, ANSI/ASHRAE Standard 55-2013. Thermal Environmental Conditions for Human Occupancy.* Atlanta: American Society of Heating Refrigerating, and Air-Conditioning Engineers, Inc.

Atmaca, I., Kaynakli, O., & Yigit, A. (2007). Effects of radiant temperature on thermal comfort. *Building and Environment*, 3210-3220.

Babiak, J., Olesen, B. W., & Petras, D. (2009). *Low Temperature Heating and High Temperature Cooling Guide Book No 7.* Rehva.

Baechler, M. C., Gilbride, T. L., Cole, P. C., Hefty, M. G., & Ruiz, K. (2015). *VOLUME 7.3 High-Performance Home Technologies: Guide to Determining Climate Regions by County.* BUILDING AMERICA BEST PRACTICES SERIES.

Bahadori, A., Zendehboudi, S., Zahedi, G., & Jamili, A. (2014). Estimation of configuration factor for radiation from a rectangle to a parallel small element of surface lying on the perpendicular to a corner of the radiator. *Chemical Engineering Communications*, 287-299.

Bean, R. (2011). Retrieved from Healthy Heating: http://www.healthyheating.com/Definitions/Mean%20Radiant_pg3.htm#.XZIrwmlKiUk

Bean, R. (2012). *Thermal Comfort: Indeed a Condition of Mind*. Retrieved from healthyheating: http://www.healthyheating.com/Thermal-Comfort-in-Simple-Terms.htm#.XlGVEShKiUk

Bean, R. (2013, February 1). *Formulas For Success*. (HPAC) Retrieved from https://www.hpacmag.com/features/formulas-for-success/

Bean, R. (2014, June 26). *Consider the human factor and building science when installing indoor climate systems.* Retrieved from Radiant & Hydronics: https://www.pmmag.com/articles/96482-consider-the-human-factor-and-building-science-when-installing-indoor-climate-systems

Benezeth, Y., Emile, B., Laurent, H., & Rosenberger, C. (2008). A Real Time Human Detection System Based on Far Infrared Vision. *Image and Signal Processing - 3rd International Conference.* Cherbourg-Octeville, France.

Bennett, D. H., Fisk, W., Apte, M. G., Wu, X., Trout, A., Faulkner, D., & Sullivan, D. (2012). Ventilation, temperature, and HVAC characteristics in small and medium commercial buildings in California. *International Journal of Indoor Environment and Health*, 309-320.

Brager, G., Zhang, H., & Arens, E. (2015). Evolving opportunities for providing thermal comfort. *Building Research & Information*, 274-287.

Budzan, S. (2015). Human Detection inThermal Images Using Low-level Features. *Measurement Automation Monitoring*.

Burt, J. E., Terjung, W. H., & O'Rourke, P. A. (1982). View-factors leading to the simulation of human heat stress and radiant exchange: An algorithm. *Theoretical and Applied Climatology*, 321-331.

Buso, T., Fabi, V., Andersen, R. K., & P.Corgnati, S. (2015). Occupant behaviour and robustness of building design. *Building and Environment*, 694 - 703.

Cannistraro, G., G.Franzitta, Giaconia, C., & Rizzo, G. (1992). Algorithms for the calculation of the view factors between human body and rectangular surfaces in parallelepiped environments. *Energy and Buildings,* 51-60.

Chang, T. Y., & Kajackaite, A. (2019). Battle for the thermostat: Gender and the effect of temperature on cognitive performance. *PLOS ONE*.

Chaudhuri, T., Soh, Y. C., Bose, S., Xie, L., & Li, H. (2016). On assuming Mean Radiant Temperature equal to air temperature during PMV-based thermal comfort study in air-conditioned buildings. *IECON 2016 - 42nd Annual Conference of the IEEE Industrial Electronics Society* (pp. 7065-7070). Florence: IEEE.

Cosma, A. C., & Simha, R. (2018). Thermal comfort modeling in transient conditions using real-time local body temperature extraction with a thermographic camera. *Building and Enviorment, 143*, 36-47.

Datcu, S., Ibos, L., Candau, Y., & Matteï, S. (2005). Improvement of building wall surface temperature measurements by infrared thermography. *Infrared Physics & Technology,* 451- 467.

Davies, M. G. (1984). An Approximate Expression for Room View Factors. *Building and Environment*, 217-219.

Derrible, S., & Reeder, M. (2015). The Cost of Over-Cooling Commercial Buildings in the United States. *Energy and Buildings*, 304-306.

Djamila, H., Chu, C.-M., & Kumaresan, S. (2014). Effect of Humidity on Thermal Comfort in the Humid Tropics. *Journal of Building Construction and Planning Research*, 35-41.

Donaisky, E., Oliveira, G. H., Freire, R. Z., & Mendes, N. (2007). PMV-Based Predictive Algorithms for Controlling Thermal Comfort in Building Plants. *2007 IEEE International Conference on Control Applications*, (pp. 182-187). Singapore.

Duan, C., Ding, X., Shi, F., Xiao, X., & Duan, P. (2011). PMV-based fuzzy algorithms for controlling indoor temperature. *2011 6th IEEE Conference on Industrial Electronics and Applications*, (pp. 1492-1496). Beijing.

Dunkle, R. V. (1963). Configuration Factors for Radiant Heat-Transfer Calcaulations Involving People. *J. Heat Transfer*, 71-76.

E.Barreira, R.M.S.F.Almeida, & Delgado, J. (2016). Infrared thermography for assessing moisture related phenomena in building components. *Construction and Building Materials*, 251-269.

Ekici, C. (2013). A Review of Thermal Comfort and Method of using Fanger's PMV Equation. *5TH International Symposium on Measurement, Analysis and Modeling of Human Functions.* Vancouver.

EmanueleNaboni, MarcoMeloni, SilviaCoccolo, JérômeKaemp, & Jean-LouisScartezzini. (2017). An overview of simulation tools for predicting the mean radiant temperature in an outdoor space. *Energy Procedia*, 1111-1116.

EricTeitelbaum, KianWeeChen, Meggers, F., HongshanGuo, Houchois, N., Pantelic, J., & Rysanek, A. (2020). Globe thermometer free convection error potentials. *Scientific Reports*.

Fanger, P. (1970). *Thermal Comfort: Analysis and Applications in Environmental Engineering.* McGraw-Hill Book Company.

Federspiel, C. C. (1998). Statistical analysis of unsolicited thermal sensation complaints in commercial buildings. *ASHRAE Transactions.* Atlanta.

FLIR. (2016). *5 Factors influencing radiometric temperature measurements.* FLIR systems.

Fokaides, P. A., Jurelionis, A., Gagyte, L., & Kalogirou, S. A. (2016). Mock target IR thermography for indoor air temperature measurement. *Applied Energy*, 676-685.

Fountain, Huizenga, M., & Charlie. (1995). *A Thermal Sensation Model for Use By The Engineering Proffession.* Berkeley, CA: ASHRAE RP-781.

Fox, M., Goodhew, S., & Wilde, P. D. (2016). Building defect detection: External versus internal thermography. *Building and Environment*, 317 - 331.

Frontczak, M., & Wargocki, P. (2011). Literature survey on how different factors influence human comfort in indoor environments. *Building and Environment*, 922-937.

G.Cannistraro, G.Franzitta, C.Giaconia, & G.Rizzo. (1992). Algorithms for the calculation of the view factors between human body and rectangular surfaces in parallelepiped environments. *Energy and Buildings*, 51-60.

Gao, G., Li, J., & Wen, Y. (2019). Energy-Efficient Thermal Comfort Control in Smart Buildings via Deep Reinforcement Learning.

Garrido, I., Lagüela, S., & Arias, P. (2018). Infrared Thermography's Application to Infrastructure Inspections. *Infrastructures*.

Gomez, A., Conti, F., & Benini, L. (2018). Thermal Image-Based CNN's for Ultra-Low Power People Recognition. *Proceedings of Low Power Embedded Systems Workshop (LP-EMS'18).* New York, NY.

Guo, H., Teitelbaum, E., Read, J., & Meggers, F. (2017). Mapping Comfort with the SMART(Spherical Motion Average Radiant Temperature) Sensor.

Haiad, C., Peterson, J., Reeves, P., Hirsch, J., & Hirsch, J. J. (2004). *Programmable Thermostats Installed into Residential Buildings: Predicting Energy Saving Using Occupant Behavior & Simulation.* Southern California Edison Design & Engineering Services.

Haiying, W., Olesen, B. W., & Kazanci, O. B. (2019). Using thermostats for indoor climate control in offices: The effect on thermal comfort and heating/cooling energy use. *Energy and Buildings*, 71-83.

Halawa, E., Hoof, J. v., & Soebarto, V. (2014). The impacts of the thermal radiation field on thermal comfort, energy consumption and control-A critical overview. *Renewable and Sustainable Energy Reviews*, 907-918.

Ham, W. d., MichelKlein, Tabatabaei, S. A., J.Thilakarathne, D., & Treur, J. (2016). Methods for a Smart Thermostat to Estimate the Characteristics of a House Based on Sensor Data. *Energy Procedia*, 467-474.

Han, J., & Bhanu, B. (2003). Detecting moving humans using color and infrared video. *Proceedings of IEEE International Conference on Multisensor Fusion and Integration for Intelligent Systems, MFI2003.*, (pp. 228-233).

Hensel, H. (1981). *Thermoreception and temperature regulation.* London: Academic Press.

Hensen, J. (1990). Literature Review on Thermal Comfort in Transient Conditions. *Building and Environment*, 309 - 316.

Horr, Y. A., Arif, M., Katafygiotou, M., Mazroei, A., Kaushik, A., & Elsarrag, E. (2016). Impact of indoor environmental quality on occupant well-being and comfort: A review of the literature. *International Journal of Sustainable Built Environment*, 1-11.

Howell, J. R. (2010). *A Catalog of Radiation Heat Transfer Configuration Factors 3rd Edition.* AUSTIN, TEXAS.

Howell, J. R., Siegel, R., & Menguc, M. P. (2011). *Thermal Radiation Heat Transfer.* CRC Press.

Hoyt, T., Arens, E., & Zhang, H. (2014). Extending air temperature setpoints: Simulated energy savings and design considerations for new and retrofit buildings. *Building and Environment*.

Hoyt, T., Arens, E., & Zhang, H. (2015). Extending air temperature setpoints: Simulated energy savings and design considerations for new and retrofit buildings. *Building and Environment*, 89-96.

Huang, J., Rathod, V., Sun, C., Zhu, M., Korattikara, A., Fathi, A., . . . Murphy, K. (2017). Speed/accuracy trade-offs for modern convolutional object detectors. *CVPR*.

Huchuk, B., O'Brien, W., & Sanner, S. (2018). A longitudinal study of thermostat behaviors based on climate, seasaonal, and energy price condiserations using connected thermostat data. *Building and Environment*, 199-210.

Huizenga, C., Abbaszadeh, S., Zagreus, L., & Arens, E. (2006). Air Quality and Thermal Comfort in Office Buildings: Results of a Large Indoor Environmental Quality Survey. *Proceedings of healthy buildings III*, 393-397.

Huizenga, C., Zhang, H., & Arens, E. (2001). A model of human physiology and comfort for assessing complex thermal environments. *Building and Environment*, 691-699.

Incropera, F. P., Dewitt, D. P., Bergman, T. L., & Lavine, A. S. (2007). *Introduction to Heat Transfer*. Wiley.

Jiang, L., Tian, F., Shen, L. E., Wu, S., Yao, S., Lu, Z., & Xu, L. (2004). Perceptual-based fusion of IR and visual images for human detection. *Proceedings of 2004 International Symposium on Intelligent Multimedia, Video and Speech Processing*, (pp. 514-517).

Jing, S., Li, B., Tan, M., & Liu, H. (2013). Impact of Relative Humidity on Thermal Comfort in a Warm Environment. *Impact of Relative Humidity on Thermal Comfort in a Warm Environment*, 598 - 607.

Jonathan, H., Rathod, V., Chow, D., Sun, C., Zhu, M., Tang, M., . . . Murphy, K. (n.d.). *tensorflow/ models*. Retrieved from Github: https://github.com/tensorflow/models/tree/master/research/object_detection

JuntaNakano, Tanabe, S.-i., & Kimura, K.-i. (2002). Differences in perception of indoor environment between Japanese and non-Japanese workers. *Energy and Buildings*, 615-621.

K.E, M. R., T.Mathew, A., & Jacob, L. (2018). A flexible control strategy for energy and comfort aware HVAC in large buildings. *Building and Environment*, 330-342.

Kalmar, F., & Kalmar, T. (2012). Interrelation between mean radiant temperature and room geometry. *Energy and Buildings*, 414-421.

Kang, D. H., Mo, P. H., Choi, D. H., Song, S. Y., Yeo, M. S., & Kim, K. W. (2010). Effect of MRT variation on the energy consumtion in a PMV-controlled office. *Building and Environment*, 1914-1922.

Kántor, N., & Unger, J. (2011). The most problematic variable in the course of human-biometeorological comfort assessment – the mean radiant temperature. *Central European Journal of Geosciences*, 90-100.

Karmann, C., Schiavon, S., & Arens, E. (2018). Percentage of commercial buildings showing at least 80% occupant satisfied with their thermal comfort. *Proceedings of 10th Windsor Conference*, (pp. 12-15). Windsor.

Karmann, C., Schiavon, S., Graham, L. T., Raftery, P., & Bauman, F. (2017). Comparing temperature and acoustic satisfaction in 60 radiant and all-air buildings. *Building and Environment*, 431-441.

Konis, K. S., & M.Annavaram. (2017). The Occupant Mobile Gateway: A participatory sensing and machine-learning approach for occupant-aware energy management. *Building and Environment*, 1-13.

Kontes, G. D., Giannakis, G. I., horn, P., Steiger, S., & Rovas, D. V. (2017). Using thermostats for Indoor Climate Control in office buildings: The effect on thermal comfort. *Energies*.

Kubaha, K., Fiala, D., & Lomas, K. (2003). Predicting human geometry-related factors for detailed radiation analysis in indoor spaces. *Eighth International IBPSA conference.* Eindhoven, Netherlands.

Kuru, M., & Calis, G. (2017). Understanding the relationship between indoor environmental parameters and thermal sensation of users via statistical analysis. *Procedia Engineering*, 808 - 815.

Kwong, Q. J., Adam, N. M., & Sahari, B. (2014). Thermal comfort assessment and potential for energy efficiency enchancement in modern tropical buildings: A review. *Energy and Buildings*, 547-557.

Kylili, A., Fokaides, P. A., Christou, P., & Kalagirou, S. A. (2014). Infrared thermography (IRT) applications for building diagnostics: A review. *Applied Energy*, 531-549.

Laguela, S., Diaz-Vilarino, L., & Roca, D. (2016). Infrared Thermography: Fundamentals and Applications. In *Non-Destructive Techniques for the Evaluation of Structures and Infrastructure* (pp. 113-138).

Langner, M., Scherber, K., & Endlicher, W. R. (2014). Indoor heat stress: An assessment of human bioclimate using the UTCI in different buildings in Berlin. *Journal of the Geographical Society of Berlin*, 260 - 273.

Levine, M. D., Ürge-Vorsatz, D., Blok, K., Geng, L., Harvey, D., Lang, S., . . . Yoshino, H. (2007). Residential and commercial buildings. In Climate Change 2007: Mitigation. Contribution of Working Group III to the Fourth Assessment Report of the Intergovernmental Panel on Climate Change [B. Metz, O.R. Davidson, P.R. Bosch, R. Dave, L.A. Meyer (eds)]. Cambridge, United Kingdom and New York, NY, USA: Cambridge University Press.

Liang, J., & Du, R. (2005). Thermal comfort control based on neural network for HVAC application. *Proceedings of 2005 IEEE Conference on Control Applications*, (pp. 819-824). Toronto.

Lucchi, E. (2018). Applications of the infrared thermography in the energy audit of buildings: A review. *Renewable and Sustainable Energy Reviews*, 3077-3090.

MacArthur, J. (1986). Humidity and predicted-mean-vote-based comfort control. *ASHRAE Trans*, (pp. 7-17).

Madsen, T. L. (1987). Measurement and control of thermal comfort in passive solar systems. *in Proc. 3rd Int. Congress on Building Energy Managment ICBEM87*, (pp. 489-496). Lausanne.

Marinetti, S., & Cesaratto, P. G. (2012). Emissivity estimation for accurate quantitative thermography. *NDT & E International*, 127-134.

Martani, C., Lee, D., Robinson, P., Britter, R., & Ratti, C. (2012). ENERNET: Studying the dynamic relationship between building occupancy and energy consumption. *Energy and Buildings*, 584 - 591.

Mendell, M. J., & Mirer, A. (2009). Indoor thermal factors and symptoms in office workers: findings from the US EPA BASE study. *International Journal of Indoor Environment and Health*.

Metzger, C. E., & Norton, P. (2014). *The Building America Indoor Temperature and Humidity Measurement Protocol.* Golden, CO: National Renewable Energy Laboratory.

Meyers, R. J., D.Williams, E., & Matthews, H. S. (2010). Scoping the potential of monitoring and control technologies to reduce energy use in homes. *Energy and Buildings*, 563 - 569.

Michelle, S., Firth, S. K., Gentry, M. I., Wright, A. J., Shipworth, D. T., & Loma, K. J. (2009). Central heating thermostat settings and timing: building demographics. *Building Research and Information*, 50-69.

Mihai, B., Wicaksono, C., Abouelenien, M., erez-Rosas, V. P., Mihalcea, R., & Ta, Y. (2014). Multimodal Sensing of Thermal Discomfort for Adaptive Energy Saving in Buildings. *IiSBE NET ZERO, BUILT ENVIRONMENT*, 344.

Mikron Instrument Company, I. (n.d.). *TABLE OF EMISSIVITY OF VARIOUS SURFACES.* Postfach: MIKRON.

Mora, R., & Bean, R. (2018). *Thermal Comfort: Designing for People.* ASHRAE Journal.

Narayana, K. (1998). View Factors for Parallel Rectangular Plates. *Heat Transfer Engineering*, 59-63.

Nevius, M. (2000). Programmable thermostats that go beserk: taking a social perspective on space heating in Wisconsin. *in proceedings of the ACEEE Summer Study on Energy Efficiency in Buildings*, (pp. 233-244).

Ng, J. J. (2019, June). *Investigating Smart Thermostat Data And Its Potential (Master's Theses)*. Retrieved from http://hdl.handle.net/1807/96163

Noémi Kántor, J. U. (2011). The most problematic variable in the course of human-biometeorological comfort assessment – the mean radiant temperature. *Central European Journal of Geosciences*, 90-100.

Olesen, B., & Parsons, K. (2002). Introduction to thermal comfort standards and to the proposed new version of EN ISO 7730. *Energy and Buildings*, 537 - 548.

Omer, K., & Kilic, M. (2005). Investigation of indoor thermal comfort under transient conditions. *Building and Environment*, 165 - 174.

Pablo, A., Salmerón, J. M., Ruiz, Á., Sánchez, F. J., & Brotas, L. (2016). The globe thermometer in comfort and environmental studies in buildings. *Revista de la construcción*, 57-66.

Palmer, J. M., & Chapman, K. S. (2000). *Direct calculation of mean radiant temperature using radiant intensities.* ASHRAE Transactions.

Park, H., & Rhee, S.-B. (2018). IoT-Based Smart Building Environment Service for Occupants' Thermal Comfort. *Journal of sensors*.

Pavlin, B., Pernigotto, G., Cappelletti, F., Bison, P., Vidoni, R., & Gasparella, A. (2017). Real-Time Monitoring of Occupant's Thermal Comfort through Infrared Imaging: A Preliminary Study. *Buildings 7*, 1.

Porras-Amores, C., Mazarron, F. R., & Canas, I. (2013). Using quantitative infrared thermography to determine indoor air temperature. *Energy and Buildings*, 292-298.

Pritoni, M., Meier, A. K., Aragon, C., Perry, D., & Peffer, T. (2015). Energy efficiency and the misuse of programmable thermostats: The effectiveness of crowdsourcing for understanding household behavior. *Energy Research & Social Science*, 190-197.

Pritoni, M., Salmon, K., Sanguinetti, A., Morejohn, J., & Modera, M. (2017). Occupant thermal feedback for improved efficiency in university. *Energy and Buildings*, 241-250.

PythonProgramming.net. (n.d.). *Introduction and Use - Tensorflow Object Detection API Tutorial*. Retrieved from pythonprogramming.net: https://pythonprogramming.net/introduction-use-tensorflow-object-detection-api-tutorial/

Ranjan, J., & Scott, J. (2016). ThermalSense: Determining Dynamic Thermal Comfort Preferences using Thermographic Imaging. *Proceedings of the 2016 ACM International Joint Conference on Pervasive and Ubiquitous Computing, UbiComp '16, ACM, New York, NY, USA*, 1212-1222.

Reddy, T. A., Kreider, J. F., Curtiss, P. S., & Rabl, A. (2017). *Heating and Cooling of Buildings Principles and Practice of Energy Efficient Design.* CRC Press.

REHVA. (2009). *Low temperature heating and high temperature cooling : embedded water surface heating and cooling systems.* Federation of European Heating and Air-Conditioning Associations.

Rinaldi, A., Schweiker, M., & Lannone, F. (2018). On uses of energy in buildings: Extracting influencing factors of occupant behaviour by means of a questionnaire survey. *Energy and Buildings*, 298 - 308.

Rossano, A., M.Tonelli, A., & Chiogna, M. (2015). A comprehensive experimental approach for the validation of quantitative infrared thermography in the evaluation of building thermal transmittance. *Applied Energy,* 218-228.

Ruben, U., Venegas, P., Guerediaga, J., Vega, L., Molleda, J., & Bulnes, F. G. (2014). Infrared Thermography for Temperature Measurement and Non-Destructive Testing. *Sensors*, 12305-12348.

Rupp, R. F., Vásquez, N. G., & Lamberts, R. (2015). A review of human thermal comfort in the built environment. *Energy and Buildings*, 178-205.

Scheatzle, D. G. (1991). The development of PMV-based control for a residence in a hot and arid climate. *ASHRAE Trans*, (pp. 1002-1019).

Shah, A. (2019, Jan 4). *Object Detection in Infrared*. Retrieved from Medium: https://medium.com/@anuj_shah/object-detection-in-infrared-3f247dc3708

Srivajana, W. (2003). Effects of Air Velocitv on Thermal Comfort in Hot and Humid Climates. *Thammasat Int J Sci Tech*.

Sun, K., & Hong, T. (2017). A simulation approach to estimate energy savings potential of occupant behavior measures. *Energy and Buildings*, 43 - 62.

Sutton, J. (2017, October 26). Retrieved from Algorithmia : https://blog.algorithmia.com/deep-dive-into-object-detection-with-open-images-using-tensorflow

Syafril, B., Yashiro, T., Khan, M. F., Koshizuka, N., & Sakamura, K. (2015). Predicting Collective User Preference for Optimal Comfort Level in Smart Buildings. *IEEE 4th Global Conference on Consumer Electronics.*

Tanabe, S., Kimura, K., & Hara, T. (1987). Thermal Comfort Requirements During the Summer Season in Japan. *ASHRAE Transactions*, 564-577.

Teitelbaum, E., Chen, K. W., Meggers, F., Guo, H., Houchois, N., Pantelic, J., & Rysanek, A. (2020). Globe thermometer free convection error potentials. *Scientific Reports*.

Tejedor, B., Casals, M., MartaGangolells, & Roca, X. (2017). Quantitative internal infrared thermography for determining in-situ thermal behaviour of façades. *Energy and Buildings*, 187-197.

Thomson, M. C., Garcia-Herrera, R., & Beniston, M. (2008). *Physiological Equivalent Temperature as Indicator for Impacts of Climate Change on Thermal Comfort of Humans.* Springer Netherlands: in Seasonal Forecasts Climatic Change and Human Health.

Thorsson, S., Lindberg, F., Eliasson, I., & Holmer, B. (2007). Different methods for estimating the mean radiant temperature in an outdoor urban setting. *International Journal of Climatology*, 1983-1993.

Tim, T., Counsell, J., & Gill, S. (2013). Energy efficiency is more than skin deep: Improving construction quality control in new-build housing using thermography. *Energy and Buildings*, 222-231.

Tom, S. (2008). Managing Energy And Comfort. *ASHRAE Journal*.

Tommaso, S. (2019). *Set-up and calibration of a test room for Indoor Environmental Quality analysis.* UNIVERSITÀ DEGLI STUDI DI PADOVA.

Tredre, B. E. (1965). Assessment of Mean Radiant Temperature in Indoor Environments . *British Journal of Industrail Medicine*, 58-66.

Tse, W., & So, A. (2000). Implementation of comfort-based air-handling unit control algorithms. United States.

U.S. Department of Energy. (2019). *EnergyPlus™ Version 9.2.0 Documentation Input Output Reference.* U.S. Department of Energy.

U.S. Department of Energy Office of Energy Efficiency and Renewable. (2004). *Buildings Energy Databook.*

U.S. Energy Information Administration. (2016, May). *Commercial Buildings Energy Consumption Survey.* Office of Energy Consumption and Efficiency Statistics. Retrieved from EIA.gov: https://www.eia.gov/consumption/commercial/data/2012/bc/cfm/b24.php

Vargas-Salgado, C., Chiñas-Palacios, C., Aguila-León, J., & Alfonso-Solar, D. (2019). Measurement of the black globe temperature to estimate the MRT and WBGT indices using a smaller diameter globe than a standardized one: Experimental analysis. *5th Carpe Conference.* Valencia.

Virote, J., & Silva, R. N. (2012). Stochastic models for building energy prediction based on occupant behavior assessment. *Energy and Buildings*, 183 - 193.

Walikewitz, N., Jänicke, B., Langner, M., Meier, F., & Endlicher, W. (2015). The difference between the mean radiant temperature and the air temperature within indoor environments: A case study during summer conditionss. *Building and Environment*, 151-161.

Winiarski, D., Halverson, M., & Jiang, W. (2007). *PNNL's CBECS Study: Analysis of Building Envelope Construction in 2003 CBECS Buildings.* Pacific Northwest National Laboratory.

Winiarski, D., Jiang, W., & Halverson, M. (2006). *PNNL's CBECS Study: Review of Pre- and Post-1980 Buildings in CBECS – HVAC Equipment.* Pacific Northwest National Laboratory.

Woods, L. D. (2018). *Model Guided Control of Radiant Slabs for Comfort abd Efficiency (Dissertation)*.

Yan, D., Brien, W. O., Hong, T., Feng, X., Gunay, H. B., Tahmasebi, F., & Mahdavi, A. (2015). Occupant behavior modeling for building performance simulation: Current state and future challenges. *Energy and Buildings*, 264 - 278.

Yang, L., Yan, H., & Lam, J. C. (2014). Thermal comfort and building energy comsumption implications - A review. *Applied Energy*, 164-173.

Zang, M., Xing, Z., & Tan, Y. (2019). IoT-based personal thermal comfort control for livable environment. *International Journal of Distributed Sensor Networks*.

Zhang, H., Arens, E., Fard, S. A., Huizenga, C., Paliaga, G., Brager, G. S., & Zagreus, L. (2007). Air movement preferences observed in office buildings. *International Journal of Biometeorology*, 349-360.

Zhang, H., Bauman, F., Arens, E., Zhai, Y., Dickerhoff, D., Zhou, X., & Luo, M. (2018). Reducing building over-cooling by adjusting HVAC supply airflow setpoints and providing personal comfort systems. *The 15th Conference of the International Society Indoor Air Quality & Climate (ISUAQ).* Philadelphia, PA, USA.

Zhao, Y., Genovese, P. V., & Li, Z. (2020). Intelligent Thermal Comfort Controlling System for Buildings Based on IoT and AI. *Future Internet*.

Zhe Wang, M. L., Zhang, H., He, Y., Jin, L., Arens, E., & Liu, S. (2018). The Effect of a Low-Energy Wearable Thermal Device on Human Comfort. *The 15th Conference of the International Society of Indoor Air Quality & Climate (ISIAQ).*

Zhou, H., Qiao, L., Jiang, Y., Sun, H., & Chen, Q. (2016). Recognition of air-conditioner operation from indoor air temperature and relative humidity by a data mining approach. *Energy and Buildings*, 233 - 241.